REPORT DOCUMENTATION PAGE

AFRL-SR-AR-TR-07-0466

PLEASE DO NOT RETURN YOUR FORM TO THE ABOVE ORGANIZATION.

1. REPORT DATE *(DD-MM-YYYY)*	2. REPORT TYPE	3. DATES COVERED *(From - To)*
	FINAL REPORT	15 JUL 2004 - 14 JUL 2007

4. TITLE AND SUBTITLE

(DEPSCORP FY04) A RESEARCH PROGRAM ON THE ASYMPTOTIC DESCRIPTION OF ELECTROMAGNETIC PULSE PROPAGATION IN SPATIALLY INHOMOGENEOUS, TEMPORALLY DISPERSIVE, ATTENUATIVE MEDIA

5a. CONTRACT NUMBER

5b. GRANT NUMBER

FA9550-04-1-0447

5c. PROGRAM ELEMENT NUMBER

61103F

6. AUTHOR(S)

PROFESSOR OUGHSTUN

5d. PROJECT NUMBER

5094/BS

5e. TASK NUMBER

5f. WORK UNIT NUMBER

7. PERFORMING ORGANIZATION NAME(S) AND ADDRESS(ES)

UNIVERSITY OF VERMON
85 SOUTH PROSPECT STREET
BURLINGTON VT 05405

8. PERFORMING ORGANIZATION REPORT NUMBER

9. SPONSORING/MONITORING AGENCY NAME(S) AND ADDRESS(ES)

AF OFFICE OF SCIENTIFIC RESEARCH
875 NORTH RANDOLPH STREET ROOM 3112
ARLINGTON VA 22203
DR ARJE NACHMAN /NE

10. SPONSOR/MONITOR'S ACRONYM(S)

11. SPONSOR/MONITOR'S REPORT NUMBER(S)

12. DISTRIBUTION/AVAILABILITY STATEMENT

DISTRIBUTION STATEMEN A: UNLIMITED

13. SUPPLEMENTARY NOTES

14. ABSTRACT

The results of this analysis have direct, meaningful application to the analysis and design of low-observable surfaces (for stealth airframes) and ultrawideband radar systems (for observing stealth airframes), the remote detection of buried structures (such as landmines and IED's), ionospheric pulse propagation (for remote sensing from an orbiting satellite), as well as the problem of ultrawideband electromagnetic pulse exposure of biological tissues. Of further interest is the application of this theory to undersea communications systems, terahertz optical communication and integrated optics systems, and the remote sensing of geophysical structures.

15. SUBJECT TERMS

16. SECURITY CLASSIFICATION OF:			17. LIMITATION OF ABSTRACT	18. NUMBER OF PAGES	19a. NAME OF RESPONSIBLE PERSON
a. REPORT	b. ABSTRACT	c. THIS PAGE			19b. TELEPHONE NUMBER *(Include area code)*

FINAL TECHNICAL REPORT
USAF Grant # FA9550-04-1-0447

A Research Program on The Asymptotic Description of Electromagnetic Pulse Propagation In Spatially Inhomogeneous, Temporally Dispersive, Attenuative Media

(July 15, 2004 – August 31, 2007)

Kurt E. Oughstun
Principal Investigator
Professor of Engineering & Mathematics
School of Engineering
College of Engineering & Mathematical Sciences
University of Vermont
Burlington, Vermont 05405-0156

September 2007

This DEPSCoR/AFOSR sponsored research grant has been used to continue the long-term support of our graduate level research program on the asymptotic description of ultrawideband signal, ultrashort pulse electromagnetic wave propagation in causally dispersive media and waveguiding systems, extending it to include the properties of spatial inhomogeneity. Our long-term research goal in this important area is to develop a rigorous, uniform asymptotic description of ultrawideband electromagnetic pulsed beam propagation, reflection, and transmission phenomena in both lossy dielectric and conducting dispersive media that may also exhibit additional complicating behavior such as either spatial inhomogeneity or spatial dispersion that is valid for arbitrarily short rise-time pulses. The results of this analysis have direct, meaningful application to the analysis and design of low-observable surfaces (for stealth airframes) and ultrawideband radar systems (for observing stealth airframes), the remote detection of buried structures (such as landmines and IED's), ionospheric pulse propagation (for remote sensing from an orbiting satellite), as well as the problem of ultrawideband electromagnetic pulse exposure of biological tissues. Of further interest is the application of this theory to undersea communications systems, terahertz optical communication and integrated optics systems, and the remote sensing of geophysical structures.

This AFOSR sponsored research program has served to provide partial support for my research colleague Dr. Natalie Cartwright as a Research Associate Professor in the Department of Mathematics at the University of Vermont during the final two years of this grant (2006-2007) following

the successful completion of her Ph.D. degree in 2004. A copy of her dissertation "Uniform Asymptotic Description of the Unit Step Function Modulated Sinusoidal Signal" was reprinted in the University of Vermont ECE/04/05-01 Research Report that was submitted with my 2004 Final Technical report. The paper "Uniform Asymptotics Applied to Ultrawideband Pulse Propagation", based upon her dissertation, is scheduled to be published in SIAM Review in November of this year. This important work completes the uniform asymptotic description of dispersive pulse propagation in a Lorentz model dielectric, a problem that was initiated by Arnold Sommerfeld in 1907 and by Leon Brillouin in 1914, was revisited by Baerwald in 1930, Stratton in 1941, Oughstun and Sherman in 1988, and finally completed by Cartwright and Oughstun in 2007, a mere century after Sommerfeld's first publication regarding the mathematically proper solution to this fundamental problem. The asymptotic solution to the ionospheric propagation problem, including the effects of spatial inhomogeneity, is currently being pursued by Professor Cartwright at SUNY-New Paltz under a separate AFOSR Young Investigator Research award. This challenging research direction is a result of the research developed under this grant and is being conducted with my collaborative support.

As a product of this funded research, the following papers were published:

1. K. E. Oughstun and N. A. Cartwright, "Physical Significance of the Group Velocity in Dispersive, Ultrashort Gaussian Pulse Dynamics," *Journal of Modern Optics* **52**, 8, 1089-1104 (2005).
2. K. E. Oughstun, "Dynamical Evolution of the Brillouin Precursor in Rocard-Powles-Debye Model Dielectrics," *IEEE Transactions on Antennas and Propagation* **53**, 5, 1582-1590 (2005).
3. K. E. Oughstun, "Several Controversial Topics in Contemporary Optics: Dispersive Pulse Dynamics and the Question of Superluminal Pulse Velocities," in *Masters in Optics: A Tribute to Emil Wolf* (SPIE Press, 2005) pp.421-453.
4. K. E. Oughstun and R. A. Albanese, "Magnetic Field Contribution to the Lorentz Model," Journal of the Optical Society of America **A 23**, 7, 1751-1756 (2006).
5. N. A. Cartwright and K. E. Oughstun, "Uniform Asymptotics Applied to Ultrawideband Pulse Propagation," SIAM Review 49, 4, xxx-xxx (2007).
6. N. A. Cartwright and K. E. Oughstun, "Ultrawideband Pulse Propagation through a Lossy Plasma," Radio Science (in preparation).

Copies of these published papers are attached at the back of this report. Reprints have already been sent to both Dr. Arje Nachman at AFOSR and to Dr. Richard Albanese at Brooks City Base at the time each publication appeared.

In addition, the following conference and workshop presentations were given during the period of this grant support:

1. K. E. Oughstun, R. A. Albanese and J. Penn, "Trapezoidal Envelope Pulse Dynamics in Debye Model Dielectrics," 2005 AFOSR Electromagnetics Workshop (January 5-7, 2005, San Antonio, Texas).
2. N. A. Cartwright and K. E. Oughstun, "Uniform Asymptotic Description of the Main Signal Arrival in Dispersive Pulse Propagation," 2006 AFOSR Electromagnetics Workshop (January 11-13, 2006, San Antonio, Texas).
3. N. A. Cartwright and K. E. Oughstun, "Uniform Asymptotic Description of the Main Signal," 2006 USNC/URSI National Radio Science Meeting, (January 4-7, 2006, University of Colorado, Boulder, CO).
4. N. A. Cartwright and K. E. Oughstun, "Ultrawideband Pulse Propagation: The Signal Contribution," AMS Joint Mathematics Meeting (San Antonio, Texas).
5. N. A. Cartwright and K. E. Oughstun, "Uniform Signal Contribution of the Step Function Modulated Sine Wave," Progress in Electromagnetics Research Symposium (PIERS 2006) (March 26-29, 2006, Cambridge, MA).
6. N. A. Cartwright and K. E. Oughstun, "Uniform Asymptotic Description of the Main Signal Contribution in Dispersive Pulse Propagation," Northern Optics 2006 (June 14-16, 2006, Bergen, Norway).
7. K. E. Oughstun and N. A. Cartwright, "Dynamical Pulse Evolution in the weak Dispersion Limit," Eightennth Annual AFOSR Electromagnetics Workshop (January 9-11, 2007, San Antonio, Texas).
8. K. E. Oughstun, "Propagation through Dispersive, Absorptive Media," AFOSR Workshop on Electromagnetic Wave Propagation through Challenging Media (May 8-9, 2007, Hanscom AFB).
9. N. A. Cartwright and K. E. Oughstun, "Ultrawideband Pulse Penetration in a Debye Medium with Static Conductivity," Fourth IASTED International Conference on Antennas, Radar, and Propagation (May 30-June 1, 2007, Montreal, Canada).
10. N. A. Cartwright and K. E. Oughstun, "Ultrawideband Pulse Penetration in an Isotropic Collisionless Plasma," 2007 CNC/USNC North American Radio Science Meeting (July 22-26, 2007, Ottawa, Canada).
11. K. E. Oughstun, "Optimal Pulse Penetration through Dielectric Barriers," 2007 CNC/USNC North American Radio Science Meeting (July 22-26, 2007, Ottawa, Canada).
12. K. E. Oughstun and N. A. Cartwright, "Ultrashort Electromagnetic Pulse Dynamics in the Singular and Weak Dispersion Limits," Progress in Electromagnetics Research Symposium (PIERS 2007) (August 27-30, 2007, Prague, Czech Republic).

Finally, the first volume of my two volume work *Electromagnetic and Optical Pulse Propagation 1: Spectral Representations in Temporally Dispersive Media* on time-domain electromagnetics was published in the Springer Series in Optical Sciences in 2006. The Preface in this book states that "the critical, long-term support of this research by Dr. Arje Nachmann at the Physics and Electronics Directorate of the United States Air Force Office of Scientific Research is gratefully acknowledged." The second volume *Electromagnetic and Optical Pulse Propagation 2: Temporal Pulse Dynamics in Dispersive, Attenuative Media* is near completion.

Journal of Modern Optics
Vol. 52, No. 8, 20 May 2005, 1089–1104

Taylor & Francis
Taylor & Francis Group

Physical significance of the group velocity in dispersive, ultrashort gaussian pulse dynamics

KURT E. OUGHSTUN* and NATALIE A. CARTWRIGHT
College of Engineering and Mathematics,
University of Vermont, Burlington, VT 05405, USA

(*Received 16 February 2004; in final form 26 April 2004*)

The properties of ultrashort gaussian pulse propagation in a dispersive, attenuative medium are reviewed with emphasis on the pulse velocity. Of particular interest is the group velocity whose physical interpretation loses meaning in causally dispersive materials as the temporal pulse width decreases into the ultrashort pulse regime. A generalized definition of the group velocity that applies to ultrashort pulses in causally dispersive materials is provided by the centroid velocity of the pulse Poynting vector whose properties are described here. In particular, it is shown that this physical velocity measure approaches the group velocity for any value of the initial pulse carrier frequency and at any fixed value of the propagation distance in the limit as the initial pulse width increases indefinitely. This then provides a convenient measure for determining when the group velocity approximation is valid.

1. Introduction

The interrelated problems of dispersive wave propagation and the group velocity have a long and involved history. In 1839, Sir William R. Hamilton [1] considered dispersive wave propagation as a coherent superposition of monochromatic scalar wave disturbances, introducing the concept of group velocity and comparing it to the phase velocity. Lord Rayleigh [2] mistakenly attributed the original definition of the group velocity to Stokes [3], stating that '*when a group of waves advances into still water, the velocity of the group is less than that of the individual waves of which it is composed; the waves appear to advance through the group, dying away as they approach its anterior limit. This phenomenon was, I believe, first explained by Stokes, who regarded the group as formed by the superposition of two infinite trains of waves, of equal amplitudes and of nearly equal wavelengths, advancing in the same direction*'. Rayleigh [4] then used these results to explain the difference in observability of the phase and group velocities.

The distinction between signal and group velocities originated in the early research of Voigt [5, 6] and Ehrenfest [7] on elementary dispersive waves, and by Laue [8] who first considered dispersive wave propagation in a region of anomalous dispersion where the absorption is both large and strongly frequency dependent. The distinction between front and signal velocities was then considered by Sommerfeld [9, 10] who proved that no signal could travel faster than the vacuum speed of light

*Corresponding author. E-mail: oughstun@emba.uvm.edu

Journal of Modern Optics
ISSN 0950-0340 print/ISSN 1362-3044 online
http://www.tandf.co.uk/journals
DOI: 10.1080/09500340512331323466

The first experimental measurement of the signal velocity was attempted by Shiren [21] in 1962 using pulsed microwave ultrasonic waves within a narrow absorption band. A more detailed analysis of these experimental results by Weber and Trizna [22] indicated that the velocity measured by Shiren was in reality that for the first precursor and not the signal. Subsequent research by Handelsman and Bleistein [23] in 1969 provided a uniform asymptotic description of the arrival and initial evolution of the signal front. The first experimental measurements of the precursor fields originally described by Sommerfeld [10] and Brillouin [12, 13] were then published by Pleshko and Palócz [24] who first referred to the first and second precursors as the Sommerfeld and Brillouin precursors, respectively. Their experimental results established the physical propriety of the asymptotic approach.

The establishment of the equivalence between the group velocity and the energy transport velocity in loss-free media [25–27] provided a physical basis for the group velocity in lossless systems. The precise formulation of the quasimonochromatic or slowly-varying envelope approximation by Born and Wolf [28] in the context of partial coherence theory then completed the mathematical and physical basis for the group velocity approximation, which was then generalized [29] and extended [30, 31] to any order of dispersion. The *quasimonochromatic or slowly-varying envelope approximation* is a hybrid time and frequency domain representation [32] in which the temporal field behaviour is separated into the product of a temporally slowly varying envelope function and an exponential phase term whose angular frequency is centred about some characteristic frequency ω_c of the pulse. The envelope function is assumed to be slowly varying on the time scale $\Delta t_c \sim 1/\omega_c$, which is equivalent [33] to the assumption that its spectral bandwidth $\Delta\omega$ satisfies the inequality $\Delta\omega/\omega_c \ll 1$. The frequency dependence of the wavenumber may then be approximated by the first few terms of its Taylor series expansion about the characteristic pulse frequency ω_c with the assumption [30–32] that improved accuracy can always be obtained through the inclusion of higher-order terms; this assumption has been proven incorrect [34–35], optimal results being obtained using either the quadratic or the cubic dispersion approximation of the wavenumber.

The description of the velocity of energy transport through a causally dispersive medium [12, 13] was reinvestigated by Schulz-DuBois [36] in 1969 and finally by Loudon [37] in 1970 who provided a correct description of the energy velocity in a single resonance Lorentz model dielectric. This description and its extension [38] to a multiple resonance Lorentz model dielectric showed that the energy velocity and group velocity are different in the region of anomalous dispersion. Based upon this critical result, Sherman and Oughstun [39, 40] then presented a complete physical description of dispersive pulse dynamics in a causally dispersive medium in terms of the energy velocity and attenuation of time-harmonic waves. This description reduces to the approximate group velocity description in the limit as the material loss goes to zero. A precise description of the signal velocity was then given by Oughstun and Sherman [41] in 1988 in connection with the modern asymptotic theory of dispersive pulse propagation [41–44]. The physical propriety and related observability of this signal velocity definition was then demonstrated [44, 45] through a numerical experiment, thereby completing the physical interpretation of the asymptotic description.

It is clear that a more physically meaningful pulse velocity measure needs to be considered in order to accurately describe the complicated pulse evolution that occurs in ultrashort dispersive pulse dynamics. One possible measure is given by the

In the asymptotic theory of dispersive pulse propagation [12, 44] the integral representation given in equation (1) is expressed as

$$A(z,t) = \frac{1}{2\pi}\int_C \tilde{f}(\omega)\exp\left[(\Delta z/c)\phi(\omega,\theta)\right]\,\mathrm{d}\omega \tag{5}$$

with *complex phase function*

$$\phi(\omega,\theta) \equiv \mathrm{i}\frac{c}{\Delta z}\left[\tilde{k}(\omega)\Delta z - \omega t\right] = \mathrm{i}\omega[n(\omega) - \theta] \tag{6}$$

and non-dimensional *space–time parameter* $\theta \equiv ct/\Delta z$. The fact that this exact integral representation of the propagated optical wave field satisfies relativistic causality is expressed by the following theorem (originally proved by Sommerfeld [9, 10] for a Heaviside unit step function modulated signal in a single resonance Lorentz model dielectric and later extended [39, 44] to an arbitrary plane wave pulse in a general causally dispersive medium):

Sommerfeld's Theorem: If $f(t) = 0$ for all $t < 0$ and if $\Re\{\mathrm{i}\omega[n(\omega) - \theta]\} \to -\infty$ as $|\omega| \to \infty$ with $\Im\{\omega\} = |\omega|\sin(\vartheta)$ for arbitrarily small $\vartheta > 0$ for all $\theta < 1$, then $A(z,t) = 0$ for all $\Delta z > 0$ when $\theta < 1$.

This precise statement of the luminal arrival of the signal front then proves that any information that may be present in the signal will follow at some later space–time point with $\theta > 1$.

3. The velocities of a gaussian envelope pulse in Lorentz model dielectrics

The group velocity approximation is a hybrid time-frequency domain representation [32] in which the pulse is separated into the product of a slowly-varying envelope and an exponential phase with angular frequency centred about a characteristic frequency of the initial pulse. With the initial pulse at the plane $z = z_0$ given by $f(t) = u(t)\sin(\omega_c t + \psi)$ with envelope $u(t)$ and fixed carrier frequency ω_c, the propagated plane wave pulse is then given by the Fourier–Laplace integral representation [44]

$$A(z,t) = \frac{1}{2\pi}\,\Re\left\{\mathrm{i}\exp(-\mathrm{i}\psi)\int_C \tilde{u}(\omega-\omega_c)\exp\left\{\mathrm{i}\left[\tilde{k}(\omega)\Delta z - \omega t\right]\right\}\mathrm{d}\omega\right\} \tag{7}$$

for all $\Delta z \geq 0$, where $\psi = 0, \pi/2$ for either a cosine or sine wave carrier, respectively. Here $\tilde{u}(\omega)$ is the temporal angular frequency spectrum of the initial pulse envelope function $u(t)$. Because of its central importance in optics, a unit amplitude gaussian envelope pulse is considered here, where

$$u(t) = \exp\left(-t^2/T^2\right), \tag{8}$$

with initial full pulse width $2T > 0$ measured at the $\exp(-1)$ amplitude points. In a multiple resonance Lorentz model [11] dielectric the complex index of refraction is described by [44]

$$n(\omega) = \left(1 - \sum_{j=0}^{N}\frac{b_{2j}^2}{\omega^2 - \omega_{2j}^2 + 2\mathrm{i}\delta_{2j}\omega}\right), \tag{9}$$

In particular, the *cubic dispersion approximation*

$$\beta(\omega) \approx \beta(\omega_c) + \beta^{(1)}(\omega_c)(\omega - \omega_c) + \frac{1}{2!}\beta^{(2)}(\omega_c)(\omega - \omega_c)^2 + \frac{1}{3!}\beta^{(3)}(\omega_c)(\omega - \omega_c)^3 \quad (14)$$

is also used because the cubic term introduces a small degree of asymmetry into the propagated pulse. However, recently published research [34, 35] has established that optimal results in the global sense are obtained either with the quadratic dispersion approximation (10) or with the cubic dispersion approximation (14).

The phase velocity $v_p(\omega) \equiv \omega/\beta(\omega)$ describes the rate at which the co-phasal surfaces propagate through the dispersive medium [2]. Since the phase of a spatially coherent optical field can only be measured indirectly [52], this velocity measure does not have any separate, measurable physical meaning in spite of the fact that it plays a central role in the mathematical description of pulse dispersion, as described by the Fourier–Laplace integral representation given in equation (1). In particular, the phase velocity of a pulse is superluminal (i.e. $v_p(\omega_c) > c$) when the input pulse carrier frequency ω_c is above the uppermost absorption band of a Lorentz model dielectric, as illustrated in figure 1 for a double resonance Lorentz model dielectric when $\omega_c > \omega_3$.

The classical group velocity $v_g(\omega) \equiv (\partial\beta(\omega)/\partial\omega)^{-1}$ describes the rate at which the envelope of a group of waves travels through the dispersive medium [1–4]. As described by Rayleigh [2], a group of waves is defined as moving beats following each other in a regular pattern as, for example, that obtained from the coherent

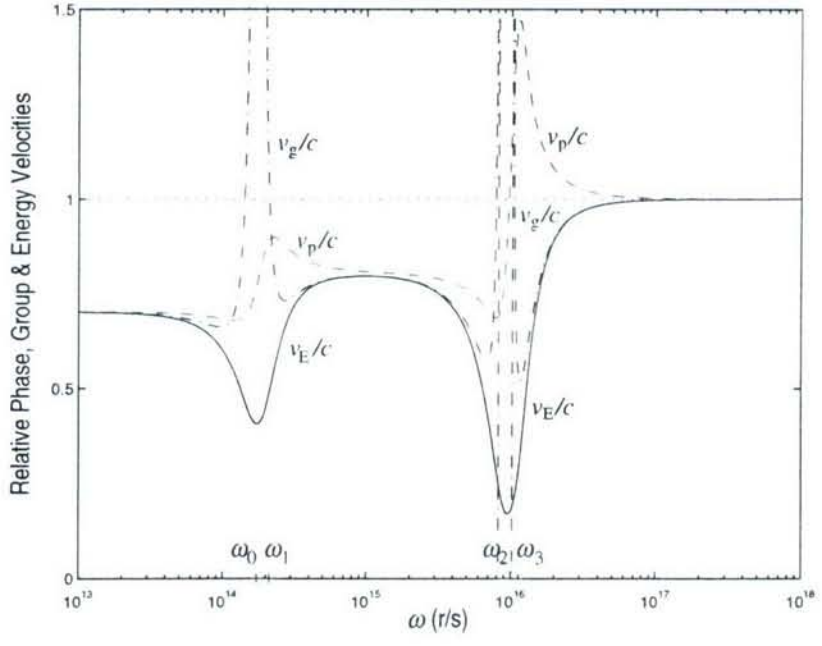

Figure 1. Angular frequency dispersion of the relative phase velocity v_p/c (dot-dashed curve), relative group velocity v_g/c (dashed curve) and relative energy velocity (solid curve) in a double resonance Lorentz model dielectric with infrared ($\omega_0 = 1.74 \times 10^{14}\,\mathrm{r\,s^{-1}}$, $b_0 = 1.22 \times 10^{14}\,\mathrm{r\,s^{-1}}$, $\delta_0 = 4.96 \times 10^{13}\,\mathrm{r\,s^{-1}}$) and near ultraviolet ($\omega_2 = 9.145 \times 10^{15}\,\mathrm{r\,s^{-1}}$, $b_2 = 6.72 \times 10^{15}\,\mathrm{r\,s^{-1}}$, $\delta_2 = 1.434 \times 10^{15}\,\mathrm{r\,s^{-1}}$) resonance lines.

corresponds to a generalized Brillouin precursor (describing the low-frequency response of the medium below the lowermost absorption band), and the field component $A_m(z, t)$, if it is present, corresponds to a generalized middle precursor (describing the intermediate-frequency response of the medium below the uppermost absorption band). A general condition for the appearance of the middle precursor is given in [42]. Each field component $A_j(z, t)$ contains a gaussian amplitude factor, the peak amplitude point of each propagating at the classical group velocity evaluated at the instantaneous oscillation frequency of that field component at that space–time point [54, 55]. As the pulse evolves, the instantaneous oscillation frequency at each peak amplitude point changes, the change being most rapid during the initial pulse evolution and in the anomalous dispersion regions where the material dispersion is greatest. If the input pulse carrier frequency ω_c is situated in a region of anomalous dispersion where the classical group velocity is either superluminal or negative (or both), then, as the pulse begins to evolve with increasing propagation distance, its instantaneous oscillation frequency at that peak amplitude point rapidly shifts into a region of normal dispersion where the group velocity is subluminal and approaches the energy transport velocity [55]. Hence, any superluminal or negative movement of the peak pulse amplitude point occurs in the initial pulse evolution and is extremely short-lived. Whether or not this motion has any physical significance is debatable as peak amplitude points in the dynamical pulse evolution are arguably not causally related [56] and may or may not convey any transfer of information [57–59]. Nevertheless, Sommerfeld's theorem clearly establishes that the front of the electromagnetic field cannot move superluminally. Since the field at some propagation distance can always be separated into two parts, one preceding a given point t_0 in time and the other following that point in time, then for all larger propagation distances, Sommerfeld's theorem states that the field part following that initial point in time cannot move ahead of the propagated space–time point $\theta_F = (c/\Delta z)(t - t_0) \equiv 1$ travelling at the speed of light c; that is, peak amplitude points at two different space–time points in the propagated field evolution that are superluminally separated are not causally connected.

It is clear that a more physically meaningful pulse velocity measure needs to be considered in order to more accurately describe the complicated pulse evolution that occurs in ultrashort dispersive pulse dynamics. One possible measure is given by the pulse centrovelocity [46]

$$v_{CE} \equiv \left| \nabla \left(\int_{-\infty}^{\infty} tE^2(\mathbf{r}, t)\, dt \Big/ \int_{-\infty}^{\infty} E^2(\mathbf{r}, t)\, dt \right)^{-1} \right|, \tag{19}$$

which describes the evolution of the temporal centre of gravity of the pulse intensity. A more appropriate velocity measure would track the temporal centroid of the Poynting vector of the pulse. This pulse centroid velocity of the Poynting vector was first introduced by Lisak [47] in 1976. Recent descriptions [48–50] of its properties have established its efficacy in describing the evolution of the pulse velocity with propagation distance in a Lorentz model dielectric.

The instantaneous centroid velocity of the pulse Poynting vector is defined as [50]

$$v_{CI} = \lim_{\Delta z \to 0} (\Delta z / \Delta \langle t \rangle) \tag{20}$$

Dynamical Evolution of the Brillouin Precursor in Rocard–Powles–Debye Model Dielectrics

Kurt Edmund Oughstun

***Abstract*—When an ultrawide-band electromagnetic pulse penetrates into a causally dispersive dielectric, the interrelated effects of phase dispersion and frequency dependent attenuation alter the pulse in a fundamental way that results in the appearance of so-called precursor fields. For a Debye-type dielectric, the dynamical field evolution is dominated by the Brillouin precursor as the propagation depth typically exceeds a single penetration depth at the carrier frequency of the input pulse. This is because the peak amplitude in the Brillouin precursor decays only as the square root of the inverse of the propagation distance. This nonexponential decay of the Brillouin precursor makes it ideally suited for remote sensing. Of equal importance is the frequency structure of the Brillouin precursor. Although the instantaneous oscillation frequency is zero at the peak amplitude point of the Brillouin precursor, the actual oscillation frequency of this field structure is quite different, exhibiting a complicated dependence on both the material dispersion and the input pulse characteristics. Finally, a Brillouin pulse is defined and is shown to possess near optimal (if not optimal) penetration into a given Debye-type dielectric.**

***Index Terms*—Electromagnetic propagation in absorbing media, electromagnetic propagation in dispersive media, electromagnetic transient propagation, ultrawideband radar.**

I. Introduction

THE dynamical evolution of an ultrawide-band electromagnetic pulse as it propagates through a causally dispersive dielectric is a classical problem [1]–[6] in electromagnetic wave theory with considerable current importance [7]–[11]. The frequency dependent phase and attenuation in a causal medium are interrelated through a Hilbert transform [12]. Because of this, an ultrawide-band pulse undergoes fundamental changes as it propagates through a dispersive material. Each spectral component travels through the dispersive medium with its own phase velocity so that the phasal relationship between the spectral components of the pulse changes with propagation distance, and each spectral component is attenuated at its own rate so that the relative amplitudes between the spectral components of the pulse also change with propagation distance. These two interrelated effects result in a complicated dynamical evolution of the propagated field [6] that is accurately described by the asymptotic theory [13]–[17] as the propagation distance exceeds a value set by the material absorption depth at the input pulse carrier frequency [18]. For an ultrawide-band pulse, these combined effects manifest themselves through the formation of well-defined precursor fields which asymptotically dominate the dynamical field behavior in the mature dispersion regime [19], [20]. Notice that an ultrawide-band pulse need not be ultrashort; for example, a rectangular envelope modulated pulse of temporal duration $T > 0$ has a spectrum that is always ultrawide-band, falling off as $|\omega|^{-1}$ as $|\omega| \to \infty$, while the pulse itself may not be ultrashort.

The precursor fields are a characteristic of the material dispersion [20], the input pulse merely providing the requisite spectral energy in the appropriate frequency domain. For the Lorentz model [21] of resonance polarization phenomena, used in the classical theory of dispersive pulse propagation [1]–[6], both a high-frequency (above resonance) Sommerfeld precursor and a low-frequency (below resonance) Brillouin precursor are present in the propagated field structure when the input pulse is ultrawideband. Additional precursor fields may also exist for a multiple resonance Lorentz model dielectric [22]. For both the Debye model [23] of orientational polarization phenomena [24] and the Rocard–Powles extension [25] of the Debye model, only the Brillouin precursor field is present in the propagated field structure [20]. Because of its unique nonexponential peak decay, the Brillouin precursor has direct application to foliage and ground penetrating radar, remote sensing and wireless communications in adverse environments. However, its efficacy depends upon its physical frequency structure about this peak amplitude point.

For carrier frequencies in the radio spectrum and below ($f_c \leq$ 300 GHz) the material response is typically dominated by orientational polarization effects [24]. Above this frequency, resonance polarization effects begin to dominate the material dispersion. The focus of this paper is on the Brillouin precursor in Rocard–Powles–Debye model dielectrics when the input ultrawide-band pulse has a carrier frequency that is sufficiently small that resonance polarization effects are entirely negligible.

II. Plane Wave Pulse Propagation in Temporally Dispersive Dielectrics

The angular frequency domain form of Maxwell's equations in source-free regions of a temporally dispersive dielectric is given by the pair of equations (with $i \equiv \sqrt{-1}$)

$$\begin{aligned} \nabla \times \tilde{\mathbf{E}}(\mathbf{r},\omega) &= i\omega\mu\tilde{\mathbf{H}}(\mathbf{r},\omega) \\ \nabla \times \tilde{\mathbf{H}}(\mathbf{r},\omega) &= -i\omega\epsilon(\omega)\tilde{\mathbf{E}}(\mathbf{r},\omega) \end{aligned} \tag{1}$$

where $\epsilon(\omega) = \epsilon_r(\omega) + i\epsilon_i(\omega)$ is the complex-valued dielectric permittivity whose real part $\epsilon_r(\omega) \equiv \Re\{\epsilon(\omega)\}$ and imaginary part $\epsilon_i(\omega) \equiv \Im\{\epsilon(\omega)\}$ form a Hilbert transform pair [12] and

Manuscript received May 8, 2003; revised November 10, 2004. This work was supported in part by the United States Air Force Office of Scientific Research (AFOSR) under Grant F49620-01-0306.

The author is with the Computational Electromagnetics Laboratory, College of Engineering and Mathematics, University of Vermont, Burlington, VT 05405-0156 USA (e-mail: oughstun@emba.uvm.edu).

Digital Object Identifier 10.1109/TAP.2005.846452

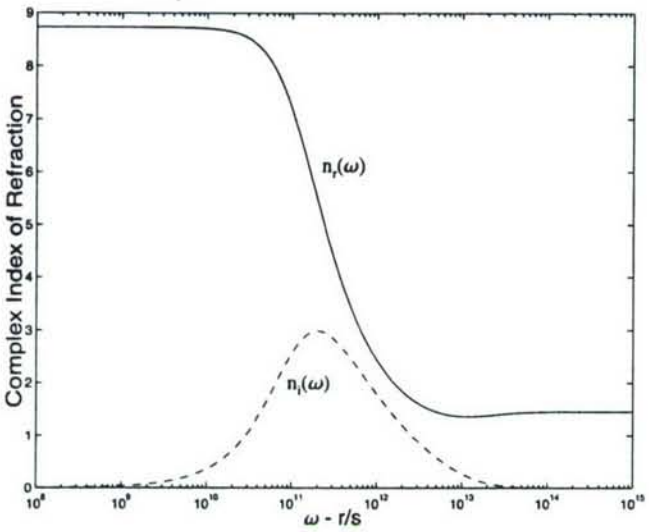

Fig. 1. Angular frequency dispersion of the real (solid curve) and imaginary (dashed curve) parts of the complex index of refraction for the simple Rocard–Powles–Debye model of triply-distilled water.

presented in this paper. The branch points of $n(\omega)$ and $\phi(\omega,\theta)$ include the singularities $\omega_{p1}=-i/\tau_f$, $\omega_{p2}=-i/\tau$ and zeroes $\omega_{z1}=-1(\tau_p-c_z)/(2\tau_m^2)$, $\omega_{z2}=-1(\tau_p+c_z)/(2\tau_m^2)$, where $\tau_p\equiv\tau+\tau_f$, $\tau_m^2\equiv\tau\tau_f$, and $c_z\equiv\sqrt{\tau_p^2-4\tau_m^2(1+a/\epsilon_\infty)}$.

For a Debye-type dielectric, the saddle point equation yields [20] just a near saddle point solution in the low-frequency domain about the origin. For $|\omega|\le|\omega_{p2}|$ the complex index of refraction (10) may be approximated by the quadratic expression

$$n(\omega)\approx\theta_0-\frac{a\tau_m^2}{2\theta_0}\left[\frac{\tau_p^2}{4\epsilon_s\tau_m^2}(\epsilon_\infty+3\epsilon_s)-1\right]\omega^2+i\frac{a\tau_p}{2\theta_0}\omega \quad (11)$$

where $\theta_0\equiv n(0)=\epsilon_s^{1/2}$. With this substitution, the saddle point equation yields, for $\theta\ge\theta_0-\kappa^2/3\zeta$, the approximate near saddle point location[1]

$$\omega_N(\theta)\approx i\frac{\kappa}{3\zeta}\left[1-\sqrt{1+\frac{3\zeta}{\kappa^2}(\theta-\theta_0)}\right] \quad (12)$$

with $\kappa\equiv a\tau_p/(2\theta_0)$ and $\zeta\equiv(a\tau_m^2/(2\theta_0))[\tau_p^2(\epsilon_\infty+3\epsilon_s)/(4\epsilon_s\tau_m^2)-1]$. Numerical results show that this saddle point moves down the imaginary axis as θ increases from the value $\theta_\infty\equiv\sqrt{\epsilon_\infty}$, crossing the origin at $\theta=\theta_0$ and then approaching the branch point singularity $\omega_{p2}=-i/\tau$ as $\theta\to\infty$, as described by (12).

[1]This approximate solution is different from the one presented in [26, eq. (21)] which is accurate only over a small space-time interval about the value θ_{RP} that is defined in that paper.

For $\theta>\theta_\infty$, the asymptotic description of the propagated field in a Debye-type dielectric may be expressed either in the form [20]

$$A(z,t)\sim A_B(z,t)+A_c(z,t) \quad (13)$$

as $\Delta z\to\infty$, or else in a form that is a superposition of expressions of the form given in (13). For example, an input rectangular envelope pulse of temporal duration T may be expressed as the difference between two Heaviside unit-step-function signals displaced in time by T, each propagated signal being described by the asymptotic expression given in (13), the first being referred to as the leading-edge signal and the latter as the trailing-edge signal. Similar representations hold for other initially symmetric pulse shapes. The field quantity $A_B(z,t)$ is due to the asymptotic contribution from the near saddle point and is referred to as the *Brillouin precursor* [20]. The field contribution $A_c(z,t)$ is due to the pole contributions (if any) and is referred to as the *signal component* [1]–[6].

The asymptotic description of the Brillouin precursor in a Rocard–Powles–Debye model dielectric is obtained through a direct application [6] of Olver's theorem [28] to the contour integral obtained from (8) by deforming the contour C to an Olver-type path through the near saddle point, with the result shown in (14) at the bottom of the page, as $\Delta z\to\infty$ with $\theta>\epsilon_\infty^{1/2}$, where $\omega_N(\theta)$ denotes the near saddle point location and where $\phi''(\omega)\equiv\partial^2\phi(\omega,\theta)/\partial\omega^2=i[2n'(\omega)+\omega n''(\omega)]$. Unlike that for a Lorentz model dielectric where there are two neighboring near saddle points that coalesce into a single second-order saddle point, thereby requiring uniform [6], [14] and transitional [29] asymptotic expansion techniques, the asymptotic expression given in (14) is uniformly valid for all finite $\theta>\epsilon_\infty^{1/2}$ provided that any pole singularities of the spectral function $\tilde{u}(\omega_N(\theta)-\omega_c)$ are sufficiently well-removed from the near saddle point location. In that case, the pole contribution $A_c(z,t)$ is given by a direct application of the residue theorem.

For example, for a Heaviside unit-step-function signal, $\tilde{u}(\omega-\omega_c)=i/(\omega_c-\omega)$ so that there is a simple pole singularity situated along the positive real frequency axis at the input carrier frequency. If θ_s denotes the space-time value when the Olver-type path $P(\theta)$ crosses the pole, then [6], [13]–[15], shown in (15) at the bottom of the following page, as $\Delta z\to\infty$ with $\theta>\epsilon_\infty^{1/2}$. The uniform asymptotic theory [6], [14], [30] describing the interaction between a saddle point and a simple pole singularity of the integrand identifies θ_s as the space-time value θ at which the steepest descent path through the near saddle point crosses the simple pole singularity at $\omega=\omega_c$.

IV. Dynamical Evolution of the Brillouin Precursor

The dynamical structure of the Brillouin precursor in a single relaxation time Rocard–Powles–Debye model dielectric when

$$A_B(z,t)\sim\Re\left\{e^{-i\psi}\left[\frac{(\frac{c}{2})\pi\Delta z}{\phi''(\omega_N(\theta))}\right]^{1/2}\tilde{u}(\omega_N(\theta)-\omega_c)\exp\left[\left(\frac{\Delta z}{c}\right)\phi(\omega_N(\theta),\theta)\right]\right\} \quad (14)$$

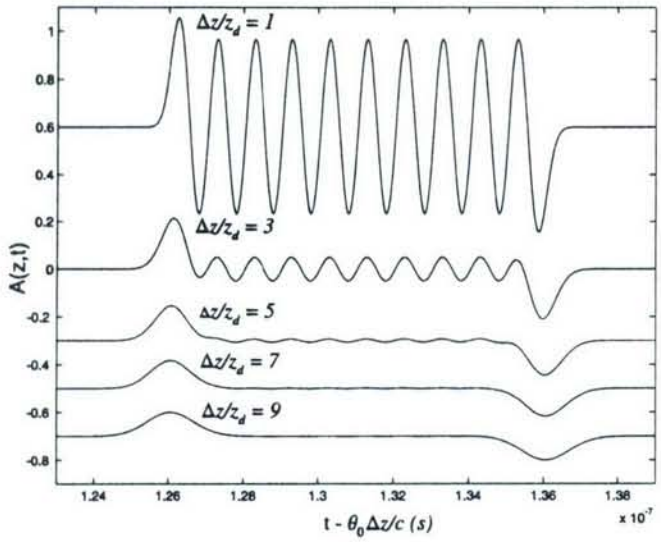

Fig. 3. Dynamical field evolution of an input unit amplitude ten cycle rectangular envelope pulse with $f_c = 1$ GHz carrier frequency at one, three, five, seven and nine absorption depths in the simple Rocard–Powles–Debye model of triply-distilled water.

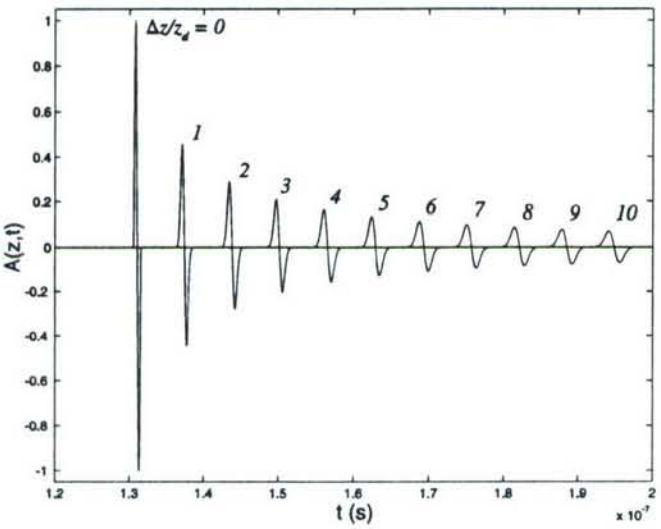

Fig. 4. Propagated pulse sequence of a unit amplitude rectangular envelope single cycle pulse with $f_c = 1$ GHz carrier frequency in the simple Rocard–Powles–Debye model of triply-distilled water.

when the propagation distance exceeds a single absorption depth at the pulse carrier frequency. This is illustrated in the sequence of graphs presented in Fig. 3 for an input ten cycle rectangular envelope pulse with 1 GHz carrier frequency and $T = 10$ ns initial pulsewidth at one, three, five, seven, and nine absorption depths in water. Notice that the leading and trailing-edge Brillouin precursors persist long after the 1 GHz signal has been significantly attenuated by the medium. Although these two Brillouin precursors penetrate very far into the material, they only carry a small fraction of the initial pulse energy in the particular case illustrated here. The leading-edge Brillouin precursor is essentially a remnant of the first half cycle of the initial pulse while the trailing-edge Brillouin precursor is a remnant of the last half cycle. The input pulse energy available to the leading and trailing-edge Brillouin precursors

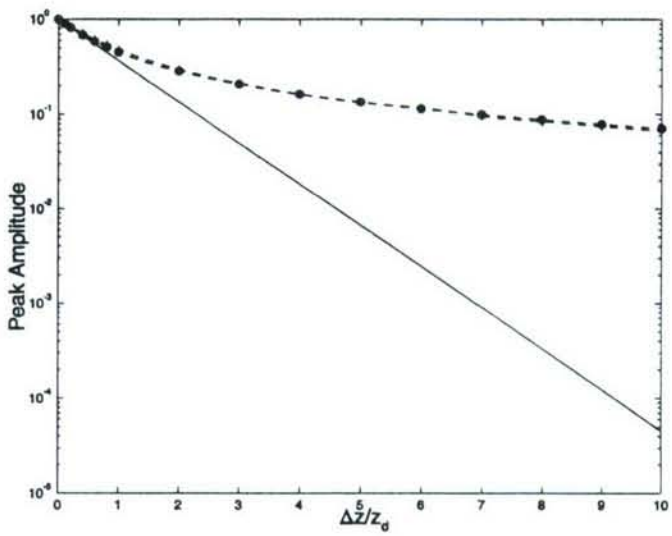

Fig. 5. Peak amplitude attenuation as a function of the relative propagation distance for input unit amplitude single cycle rectangular envelope pulses with carrier frequencies $f_c = 0.1$ GHz (* symbols), $f_c = 1$ GHz (o symbols), and $f_c = 10$ GHz (+ symbols). The solid curve describes the pure exponential attenuation given by $\exp(-\Delta z/z_d)$.

is then limited to that contained in a single cycle of the input rectangular envelope pulse. For a ten cycle pulse as illustrated in Fig. 3, this means that, at most, only ten percent of the input pulse energy is available to this precursor pair [33].

A more efficient way to generate a Brillouin precursor pair in a dispersive material is with a single cycle pulse. The pulse sequence presented in Fig. 4 illustrates the dynamical pulse evolution as a unit amplitude, rectangular envelope single cycle pulse with $f_c = 1$ GHz penetrates into water with $\Delta z/z_d = 0, 1, 2, \ldots, 10$. The evolution of the pulse into a pair of leading and trailing-edge Brillouin precursors is clearly evident as the propagation distance exceeds a single absorption depth ($\Delta z/z_d > 1$) and the peak amplitude attenuation goes from exponential decay to the $(\Delta z)^{-1/2}$ algebraic decay described in (16). This transition is illustrated in Fig. 5 which presents the peak amplitude decay as a function of the relative propagation distance $\Delta z/z_d$. The solid curve in the figure describes the behavior of the function $\exp(-\Delta z/z_d)$ which represents pure exponential decay. The numerically determined peak amplitude decay for three different input single cycle pulses with carrier frequencies $f_c = 0.1$ GHz, $f_c = 1$ GHz, and $f_c = 10$ GHz is presented in this figure by the $*$, $\circ$, and $+$ symbols, respectively, each data set connected by a cubic spline fit.

The temporal width of the leading-edge Brillouin precursor as a function of the propagation distance is illustrated in Fig. 6. Part (a) of the figure is plotted in terms of the absolute propagation distance in meters while (b) is plotted in terms of the relative propagation distance $\Delta z/z_d$. The dependence of the absorption depth $z_d = \alpha^{-1}(\omega_c)$ on the carrier frequency of the pulse is reflected in the individual curves appearing in Fig. 6(b). The solid curves in the figure describe the asymptotic result given in (20) and the three sets of data points present numerical results for the $f_c = 0.1$ GHz, $f_c = 1$ GHz, and $f_c = 10$ GHz single cycle pulse cases, each data set connected by a cubic spline fit. Notice

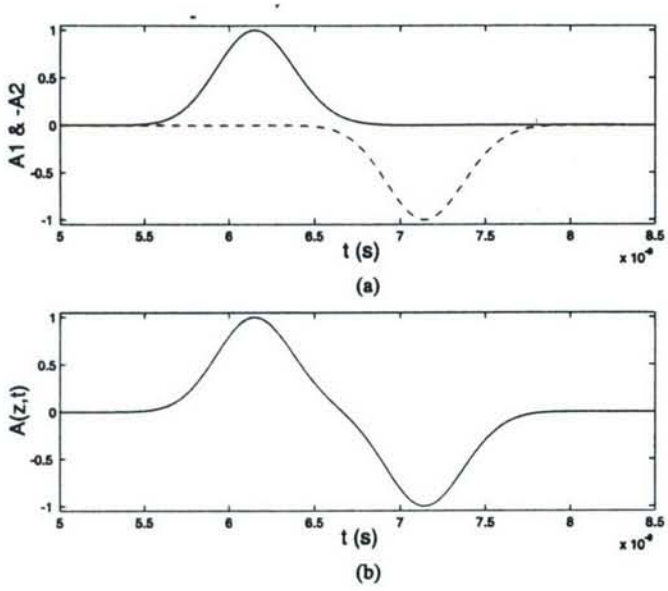

Fig. 9. Temporal structure of the Brillouin pulse *BP1* with time delay $T = 1/(2f_c)$ for $f_c = 1$ GHz. The separate leading and trailing-edge precursor components are illustrated in part (a) and their superposition is given in part (b).

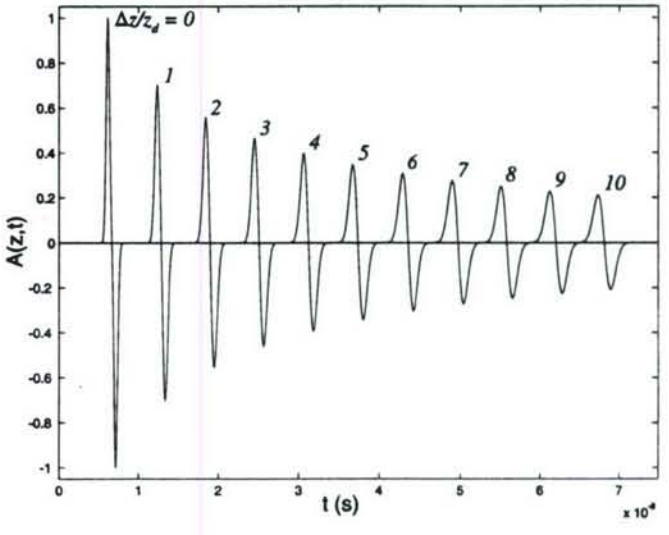

Fig. 10. Propagated pulse sequence for the Brillouin pulse *BP1* with delay time $T = 1/(2f_c)$ for $f_c = 1$ GHz in the simple Rocard–Powles–Debye model of triply-distilled water.

penetrate a finite distance into a given dispersive dielectric. The results presented in Figs. 4 and 5 indicate that the pulse that will provide near-optimal, if not indeed optimal, penetration is comprised of a pair of Brillouin precursor structures with the second precursor delayed in time and π phase shifted from the first. This so-called *Brillouin pulse* is obtained from (14) with $\Delta z = z_d = \alpha^{-1/2}(\omega_c)$ in the exponential, the other factors not appearing in the exponential set equal to unity, and is given by

$$f_{BP}(t) = \exp\left[\frac{\phi(\omega_N(\theta),\theta)}{\omega_c n_i(\omega_c)}\right] - \exp\left[\frac{\phi(\omega_N(\theta_T),\theta_T)}{\omega_c n_i(\omega_c)}\right] \quad (22)$$

where $\theta_T \equiv \theta - cT/z_d$ with $T > 0$ describing the fixed time delay between the leading and trailing-edge Brillouin precursors. If T is chosen too small then there will be significant destructive interference between the leading and trailing-edges and the pulse will be rapidly extinguished. For practical reasons, $2T$ should be chosen near to the inverse of the operating frequency f_c of the antenna used to radiate this Brillouin pulse.

With $T = 1/(2f_c)$ the input Brillouin pulse is approximately a single cycle pulse with effective oscillation frequency equal to f_c. The input Brillouin pulse when $f_c = 1$ GHz is depicted in Fig. 9; part (a) of the figure shows the separate leading and trailing-edge Brillouin precursor structures while part (b) of the figure shows the final pulse obtained from the superposition of these two parts, as described by (22). The initial rise and fall time for this pulse is ~ 0.6 ns. The dynamical evolution of this input Brillouin pulse in triply-distilled water is illustrated by the pulse sequence given in Fig. 10 with $\Delta z/z_d = 0, 1, 2, \ldots, 10$. Comparison with the pulse sequence depicted in Fig. 4 for a 1 GHz single cycle rectangular envelope pulse shows that the Brillouin pulse decays much slower with propagation distance. Improved results are obtained when the delay is doubled to the value $T = 1/f_c$. In this case there is a noticeable "dead-time" between the leading and trailing-edge Brillouin precursor structures which decreases the effects of destructive interference between these two components of the Brillouin pulse, resulting in improved penetration into the dispersive, absorptive material. However, this destructive interference can never be completely eliminated for all propagation distances since the time delay between the peak amplitude points for the leading and trailing-edge Brillouin precursors decreases with the inverse of the propagation distance [6], [15]. Nevertheless, it can be effectively eliminated over a given finite propagation distance by choosing the time delay T sufficiently large. The tradeoff in doing this is to decrease the effective oscillation frequency of the radiated pulse.

The numerically determined peak amplitude decay with relative propagation distance $\Delta z/z_d$ is presented in Fig. 11. The lower solid curve depicts the exponential attenuation described by the function $\exp(-\Delta z/z_d)$, and the lower dashed curve describes the peak amplitude decay for a single cycle rectangular envelope pulse with $f_c = 1$ GHz. Notice that the departure from pure exponential attenuation occurs when $\Delta z/z_d \approx 0.5$ as the leading and trailing-edge Brillouin precursors begin to emerge from the pulse. The dashed curve labeled *BP1* describes the peak amplitude decay for the Brillouin pulse with $T = 1/(2f_c)$, *BP2* describes that for the Brillouin pulse with $T = 1/f_c$, and *BP3* describes that for $T = 3/(2f_c)$. There is no noticeable improvement in the peak amplitude decay as the delay time T is increased beyond $3/(2f_c)$ over the illustrated range of propagation distances. Notice that at ten absorption depths, $\exp(-\Delta z/z_d) = \exp(-10) \cong 4.54 \times 10^{-5}$, the peak amplitude of the single cycle pulse is 0.0718, the peak amplitude of the Brillouin pulse *BP1* is 0.2123, the peak amplitude of the Brillouin pulse *BP2* is 0.2943, and the peak amplitude of the Brillouin pulse *BP3* is 0.3015, over three orders of magnitude larger than that expected from simple exponential attenuation.

The power associated with the observed peak amplitude decay presented in Fig. 11 may be accurately determined [34] by plotting the base ten logarithm of the peak amplitude data versus the base ten logarithm of the relative propagation distance. If the algebraic relationship between these two quantities is of the form $A_{\text{peak}} = B(\Delta z/z_d)^p$ where B is a constant, then

REFERENCES

[1] A. Sommerfeld, "Über die fortpflanzung des lichtes in disperdierenden medien," *Ann. Phys.*, vol. 44, pp. 177–202, 1914.

[2] L. Brillouin, "Über die fortpflanzung des licht in disperdierenden medien," *Ann. Phys.*, vol. 44, pp. 203–240, 1914.

[3] ——, *Wave Propagation and Group Velocity*. New York: Academic Press, 1960.

[4] J. A. Stratton, *Electromagnetic Theory*. New York: McGraw-Hill, 1941, sec. 5.12 and 5.18.

[5] J. D. Jackson, *Classical Electrodynamics*, 3rd ed. New York: Wiley, 1999, sec. 7.8–7.11.

[6] K. E. Oughstun and G. C. Sherman, *Electromagnetic Pulse Propagation in Causal Dielectrics*. Berlin-Heidelberg, Germany: Springer-Verlag, 1994.

[7] H. L. Bertoni, L. Carin, and L. B. Felsen, Eds., *Ultra-Wideband, Short-Pulse Electromagnetics*. New York: Plenum, 1993.

[8] L. Carin and L. B. Felsen, Eds., *Ultra-Wideband, Short-Pulse Electromagnetics*. New York: Plenum, 1995, vol. 2.

[9] C. E. Baum, L. Carin, and A. P. Stone, Eds., *Ultra-Wideband, Short-Pulse Electromagnetics*. New York: Plenum, 1997, vol. 3.

[10] E. Heyman, B. Melbaum, and J. Shiloh, Eds., *Ultra-Wideband, Short-Pulse Electromagnetics*. New York: Plenum, 1999, vol. 4.

[11] P. D. Smith and S. R. Cloude, Eds., *Ultra-Wideband, Short-Pulse Electromagnetics*. New York: Kluwer, 2002, vol. 5.

[12] H. M. Nussenzveig, *Causality and Dispersion Relations*. New York: Academic, 1972, ch. 1.

[13] K. E. Oughstun and G. C. Sherman, "Propagation of electromagnetic pulses in a linear dispersive medium with absorption (the Lorentz medium)," *J. Opt. Soc. Amer. B*, vol. 5, pp. 817–849, 1988.

[14] ——, "Uniform asymptotic description of electromagnetic pulse propagation in a linear dispersive medium with absorption (the Lorentz medium)," *J. Opt. Soc. Amer. A*, vol. 6, pp. 1394–1420, 1989.

[15] ——, "Uniform asymptotic description of ultrashort rectangular optical pulse propagation in a linear, causally dispersive medium," *Phys. Rev. A*, vol. 41, pp. 6090–6113, 1990.

[16] C. M. Balictsis and K. E. Oughstun, "Uniform asymptotic description of ultrashort gaussian pulse propagation in a causal, dispersive dielectric," *Phys. Rev. E*, vol. 47, no. 5, pp. 3645–3669, 1993.

[17] ——, "Generalized asymptotic description of the propagated field dynamics in gaussian pulse propagation in a linear, causally dispersive medium," *Phys. Rev. E*, vol. 55, no. 2, pp. 1910–1921, 1997.

[18] H. Xiao and K. E. Oughstun, "Failure of the group velocity description for ultrawideband pulse propagation in a double resonance Lorentz model dielectric," *J. Opt. Soc. Amer. B*, vol. 16, pp. 1773–1785, 1999.

[19] G. C. Sherman and K. E. Oughstun, "Description of pulse dynamics in Lorentz media in terms of the energy velocity and attenuation of time-harmonic waves," *Phys. Rev. Lett.*, vol. 47, pp. 1451–1454, 1981.

[20] K. E. Oughstun, "Dynamical structure of the precursor fields in linear dispersive pulse propagation in lossy dielectrics," in *Ultra-Wideband, Short-Pulse Electromagnetics*, L. Carin and L. B. Felsen, Eds. New York: Plenum, 1995, vol. 2, pp. 257–272.

[21] H. A. Lorentz, *The Theory of Electrons*. New York: Dover, 1952.

[22] S. Shen and K. E. Oughstun, "Dispersive pulse propagation in a double resonance Lorentz medium," *J. Opt. Soc. Amer. B*, vol. 6, pp. 948–963, 1989.

[23] P. Debye, *Polar Molecules*. New York: Dover, 1929.

[24] C. F. Bohren and D. R. Huffman, *Absorption and Scattering of Light by Small Particles*. New York: Wiley, 1983, ch. 8.

[25] J. McConnel, *Rotational Brownian Motion and Dielectric Theory*. London, U.K.: Academic, 1980.

[26] J. E. K. Laurens and K. E. Oughstun, "Electromagnetic impulse response of triply-distilled water," in *Ultra-Wideband, Short-Pulse Electromagnetics*, E. Heyman, B. Melbaum, and J. Shiloh, Eds. New York: Plenum, 1999, vol. 4, pp. 243–264.

[27] P. Debye, "Näherungsformeln für die zylinderfunktionen für grosse werte des arguments und unbeschränkt veranderliche werte des index," *Math. Ann.*, vol. 67, pp. 535–558, 1909.

[28] F. W. J. Olver, "Why steepest descents?," *SIAM Review*, vol. 12, pp. 228–247, 1970.

[29] J. A. Solhaug, K. E. Oughstun, J. J. Stamnes, and P. D. Smith, "Uniform asymptotic description of the Brillouin precursor in a Lorentz model dielectric," *J. Eur. Opt. Soc. A*, vol. 7, pp. 575–602, 1998.

[30] C. Chester, B. Friedman, and F. Ursell, "An extension of the method of steepest descents," *Proc. Cambridge Phil. Soc.*, vol. 53, pp. 599–611, 1957.

[31] L. Mandel, "Interpretation of instantaneous frequencies," *Am. J. Phys.*, vol. 42, pp. 840–846, 1974.

[32] K. E. Oughstun, "Noninstantaneous, finite rise-time effects on the precursor field formation in linear dispersive pulse propagation," *J. Opt. Soc. Amer. A*, vol. 12, pp. 1715–1729, 1995.

[33] P. D. Smith and K. E. Oughstun, "Electromagnetic energy dissipation and propagation of an ultrawideband plane wave pulse in a causally dispersive dielectric," *Radio Sci.*, vol. 33, pp. 1489–1504, 1998.

[34] H. J. J. Braddick, *The Physics of Experimental Method*, 2nd ed. London, U.K.: Chapman & Hall, 1963, sec. 2.9.

Kurt Edmund Oughstun received the B.A. degree *cum laude* in physics and mathematics from Central Connecticut State University, New Britain, in 1972 and the M.S. degree in optical engineering and the Ph.D. degree in optical physics from The Institute of Optics, University of Rochester, Rochester, NY, in 1974 and 1978, respectively.

Currently, he is a Professor of electrical engineering, mathematics, and computer science in the College of Engineering and Mathematics at the University of Vermont, Burlington. His research is centered on ultrawide-band time-domain electromagnetics and ultrashort optical pulse propagation in complex dispersive media.

Dr. Oughstun is a Fellow of the Optical Society of America, a Member of the European Optical Society, the United States National Committee of the International Union of Radio Science (Commission B), the National Geographic Society, and the Electromagnetics Academy. He held a Corning Foundation Fellowship in 1978. He was named University Scholar in the Basic and Applied Sciences at the University of Vermont in 1996.

Chapter 20

Several Controversial Topics in Contemporary Optics: Dispersive Pulse Dynamics and the Question of Superluminal Pulse Velocities

Kurt Edmund Oughstun
Computational Electromagnetics Laboratory
College of Engineering & Mathematics
University of Vermont
Burlington, VT 05405-0156
U. S. A.

seminal analysis, Brillouin concluded that[11,12] *"The signal velocity does not differ from the group velocity, except in the region of anomalous dispersion. There the group velocity becomes greater than the velocity in vacuum if the reciprocal c/U < 1; it even becomes negative...Naturally, the group velocity has a meaning only so long as it agrees with the signal velocity. The negative parts of the group velocity have no physical meaning...The signal velocity is always less than or at most equal to the velocity of light in vacuum."* This research then established the asymptotic theory of pulse propagation in dispersive, absorptive media. An essential feature of this approach is its' adherence to relativistic causality through careful treatment of the dispersive properties of both the real and imaginary parts of the complex index of refraction.

At approximately the same time, Havelock[14,15] completed his research on wave propagation in dispersive media based upon Kelvin's stationary phase method[16]. It appears that Havelock was the first to employ the Taylor series expansion of the wave number (κ in Havelock's notation) about a given wavenumber value κ_0 that the spectrum of the wave group is clustered about, referring to this approach as the group method. In addition, Havelock[15] stated that *"The range of integration is supposed to be small and the amplitude, phase and velocity of the members of the group are assumed to be continuous, slowly varying, functions of* κ." This research then established the group velocity method for dispersive wave propagation. Since the method of stationary phase[17] requires that the wavenumber be real-valued, this method cannot properly treat causally dispersive, attenuative media. Furthermore, notice that Havelock's group velocity method is a significant departure from Kelvin's stationary phase method with regard to the wavenumber value κ_0 about which the Taylor series expansion is taken. In Kelvin's method, κ_0 is the stationary phase point of the wavenumber κ while in Havelock's method κ_0 describes the wavenumber value about which the wave group spectrum is peaked. This apparently subtle change in the value of κ_0 results in significant consequences for the accuracy of the resulting group velocity description.

There were then two different approaches to the problem of dispersive pulse propagation: the asymptotic approach (based upon Debye's method[12] of steepest descent) which provided a proper accounting of causality but was considered to be mathematically unwieldy without any simple, physical interpretation, and Havelock's group velocity approximation (based upon Havelock's reformulation[14,15] of Kelvin's asymptotic method[15] of stationary phase) which violates causality but possesses a simple, physically appealing interpretation. It is interesting to note that both methods are based upon an asymptotic expansion technique but with two very different approaches, the method of stationary phase relying upon coherent interference and the method of steepest descent relying upon attenuation.

The asymptotic approach was revisited by Baerwald[18] in 1930 who reconsidered Brillouin's description[10,11] of the signal velocity in causally dispersive systems, and also by Stratton[19] in 1941, who reformulated the problem in terms of the Laplace transform and derived an alternate contour integral representation of the propagated signal. Stratton appears to have first referred to the forerunners described by Sommerfeld[10] and Brillouin[11,12] as precursors. The first experimental measurement of the signal velocity was attempted by Shiren[20] in 1962 using pulsed microwave ultrasonic waves within a narrow absorption band. His experimental results[20] were *"found to lie within theoretical limits established by calculations of Brillouin and Baerwald."* However, a more detailed analysis of these experimental results by Weber and Trizna[21] indicated that the velocity measured by Shiren was in reality that for the first precursor and not the signal. Subsequent research by Handelsman and Bleistein[22] in 1969 provided a uniform asymptotic description of the arrival and initial evolution of the signal front. The first experimental measurements of the

$\Delta\omega/\omega_c << 1$ is satisfied. The frequency dependence of the wavenumber may then be approximated by the first few terms of its Taylor series expansion about the characteristic pulse frequency ω_c with the assumption[35,36,50] that improved accuracy can always be obtained through the inclusion of higher-order terms; this assumption has been proven incorrect[48,49], optimal results being obtained using either the quadratic or the cubic dispersion approximation of the wavenumber.

Because of the slowly-varying envelope approximation together with the neglect of the frequency dispersion of the material attenuation, the group velocity approximation is invalid in the ultrashort pulse regime in a causally dispersive material or system, its' accuracy decreasing as the propagation distance Δz increases. This is in contrast with the modern asymptotic description whose accuracy increases in the sense of Poincaré[17] as the propagation distance increases. There is then a critical propagation distance $z_c > 0$ such that the group velocity description using either the quadratic or cubic dispersion approximation provides an accurate description of the pulse dynamics when $0 \le \Delta z < z_c$, the accuracy increasing as $\Delta z \to 0$, while the modern asymptotic theory provides an accurate description when $\Delta z > z_c$, the accuracy increasing as $\Delta z \to \infty$. This critical distance z_c depends upon both the dispersive material and the input pulse characteristics including the pulse shape, temporal width and characteristic angular frequency ω_c. For example, $z_c = \infty$ for the trivial case of vacuum for all pulse shapes, whereas $z_c \sim z_d$ for an ultrashort, ultrawideband pulse in a causally dispersive dielectric with e^{-1} penetration depth z_d at the characteristic frequency ω_c of the input pulse.

In spite of these results, the group velocity approximation remains central to the description of ultrashort pulse dynamics in both linear and nonlinear optics with little regard to its domain of validity. This is seemingly supported by the apparent agreement between experimental measurements and results predicted by the group velocity approximation. Herein lies the central controversy considered in this paper. Related to this is the controversy regarding the possibility of superluminal pulse velocities since the group velocity can assume any value between $-\infty$ and $+\infty$ in a region of anomalous dispersion.

20.2. Integral Representation of the Propagated Pulse and Causality

The propagated plane wave, pulsed optical field $A(z,t)$ that results from the initial pulse $A(z_0,t) = f(t)$ at the plane $z = z_0$ is given by the *Fourier-Laplace integral representation*[46]

$$A(z,t) = \frac{1}{2\pi}\int_C \tilde{f}(\omega) e^{i\left[\tilde{k}(\omega)\Delta z - \omega t\right]} d\omega \tag{20.1}$$

for all $\Delta z \ge 0$. Here $\tilde{f}(\omega)$ is the temporal angular frequency spectrum of the initial pulse function $f(t)$, C denotes the contour of integration $\omega = \omega' + ia$ where $\omega' = \Re\{\omega\}$ ranges from negative to positive infinity, and a is a constant greater than the abscissa of absolute convergence for $f(t)$. The spectrum $\tilde{A}(z,\omega)$ of the optical field $A(z,t)$ satisfies the *Helmholtz equation*

$$\left[\nabla^2 + \tilde{k}^2(\omega)\right]\tilde{A}(z,\omega) = 0, \tag{20.2}$$

where

20.3. Havelock's Classical Group Velocity Approximation

The group velocity approximation is a hybrid time and frequency domain representation[50] in which the temporal pulse behavior is separated into the product of a slowly-varying envelope function and an exponential phase term whose angular frequency is centered about some fixed characteristic frequency of the initial pulse. Consider then the specific form of the initial pulse at the plane $z = z_0$ that is given by $f(t) = u(t)\sin(\omega_c t + \psi)$ with envelope $u(t)$ and constant carrier frequency ω_c. The propagated plane wave pulse is then given by the Fourier-Laplace integral representation[46]

$$A(z,t) = \frac{1}{2\pi}\Re\left\{ie^{-i\psi}\int_C \tilde{u}(\omega-\omega_c)e^{i\left[\tilde{k}(\omega)\Delta z-\omega t\right]}d\omega\right\} \tag{20.7}$$

for all $\Delta z \geq 0$, where $\psi = 0, \pi/2$ for either a cosine or sine wave carrier, respectively. Here $\tilde{u}(\omega)$ is the temporal angular frequency spectrum of the initial pulse envelope function $u(t)$. In the slowly-varying envelope approximation, the envelope function $u(t)$ is assumed to be slowly-varying on the time scale $\Delta t_c \sim 1/\omega_c$, which is equivalent[51] to the quasimonochromatic approximation that the spectral bandwidth $\Delta\omega$ of $\tilde{u}(\omega)$ is sufficiently narrow that the inequality $\Delta\omega/\omega_c << 1$ is satisfied. The complex wavenumber $\tilde{k}(\omega)$ is then expanded in a Taylor series about the carrier frequency ω_c with the assumption[34-36,50] that this series may be truncated after a few terms with some undefined error. It is typically assumed that the attenuation coefficient $\alpha(\omega) = \Im\left\{\tilde{k}(\omega)\right\}$ is sufficiently small that it's frequency dispersion is entirely negligible in comparison to that for the propagation factor $\beta(\omega) = \Re\left\{\tilde{k}(\omega)\right\}$, so that $\alpha(\omega) \approx \alpha(\omega_c)$; this is entirely compatible with the stationary phase foundation[14-16] of the group velocity description which requires that the wavenumber be real-valued since this frequency independent attenuation factor may then be taken outside of the integration. In addition, the propagation factor $\beta(\omega)$ is typically represented by the *quadratic dispersion approximation*

$$\beta(\omega) \approx \beta(\omega_c) + \beta^{(1)}(\omega_c)(\omega-\omega_c) + \frac{1}{2!}\beta^{(2)}(\omega_c)(\omega-\omega_c)^2, \tag{20.8}$$

where $\beta^{(j)}(\omega) \equiv \partial^j\beta(\omega)/\partial\omega^j$. The coefficient $\beta^{(1)}(\omega_c)$ is the inverse of the *group velocity* evaluated at the carrier frequency, while the coefficient $\beta^{(2)}(\omega_c)$ describes the so-called *group velocity dispersion*[50]. With this substitution, Eq. (20.7) becomes

$$A(z,t) \approx \frac{e^{-\alpha(\omega_c)\Delta z}}{\left[2\pi\beta^{(2)}(\omega_c)\Delta z\right]^{1/2}}\Re\left\{e^{i\left[\beta(\omega_c)\Delta z-\omega_c t-\psi-3\pi/4\right]}\int_{-\infty}^{\infty}u(t')\exp\left[-i\frac{\left(\beta'(\omega_c)\Delta z+t'-t\right)^2}{2\beta^{(2)}(\omega_c)\Delta z}\right]dt'\right\}, \tag{20.9}$$

and the pulse phase propagates through the dispersive medium at the *phase velocity*

$$v_p(\omega) \equiv \frac{\omega}{\beta(\omega)}, \tag{20.10}$$

while the pulse envelope propagates through the dispersive medium at the group velocity

field. A complete understanding of these saddle point dynamics together with the manner in which they interact with the initial pulse spectrum provides a detailed, accurate description of the entire dynamical evolution of the propagated pulse in the dispersive, absorptive medium for all $\Delta z > z_c$, the accuracy of this approximation increasing in the sense of Poincaré[17] as the propagation distance increases above some critical propagation distance $z_c > 0$.

The set of saddle points of the complex phase function $\phi(\omega,\theta) = i\omega[n(\omega) - \theta]$ is determined by the condition that $\phi(\omega,\theta)$ be stationary at a saddle point, in which case $\phi'(\omega,\theta) = 0$, where the prime denotes differentiation with respect to ω, so that

$$n(\omega) + \omega n'(\omega) = \theta \quad . \tag{20.14}$$

The solutions of this saddle point equation then give the desired saddle point locations in the complex ω-plane as a function of the space-time parameter $\theta = ct/\Delta z$. The saddle points will then evolve with time at any fixed propagation distance Δz. Because of the general symmetry relations[43,46] $n(-\omega) = n^*(\omega^*)$ and $\phi(-\omega,\theta) = \phi^*(\omega^*,\theta)$ that are satisfied by a causal medium, if $\omega_j(\theta)$ is saddle point of $\phi(\omega,\theta)$, then so also is $-\omega_j^*(\theta)$.

An appreciation of the physical significance of the saddle points can be obtained from the relation $(\Delta z/c)\phi(\omega,\theta) = i\left(\tilde{k}(\omega)\Delta z - \omega t\right)$ for the complex phase function. Upon differentiating this expression with respect to ω, one obtains $(\Delta z/c)\phi'(\omega,\theta) = i\left(\left(\partial\tilde{k}(\omega)/\partial\omega\right)\Delta z - t\right)$. Since $\phi'(\omega,\theta) = 0$ at each saddle point $\omega_j(\theta)$ of ϕ, then

$$\frac{\Delta z}{t} = \frac{1}{\left(\partial\tilde{k}(\omega)/\partial\omega\right)_{\omega=\omega_j}} = \tilde{v}_g(\omega_j) \tag{20.15}$$

and the *complex group velocity* is real-valued at the saddle points.

With the saddle point locations known for $\theta \geq 1$, the asymptotic analysis then proceeds by expressing the integral representation given in Eq. (20.5) in terms of an integral $I(z,\theta)$ with the same integrand but with a new contour of integration $P(\theta)$ to which the original contour C may be deformed[43-46]. By Cauchy's residue theorem, the integral representation (20.5) of $A(z,t)$ and the contour integral $I(z,\theta)$ are related by

$$A(z,t) = I(z,\theta) - \Re\{2\pi i\Lambda(\theta)\} \quad , \tag{20.16}$$

where

$$\Lambda(\theta) = \sum_p \operatorname{Res}_{\omega=\omega_p}\left\{\frac{1}{2\pi}\tilde{f}(\omega)\exp[(\Delta z/c)\phi(\omega,\theta)]\right\} \tag{20.17}$$

is the sum of the residues of the poles that were crossed in the deformation from C to $P(\theta)$, and where

values of $z > z_0$ for sufficiently large t. As a result, this contribution to the asymptotic behavior of the propagated field describes the steady-state behavior of the signal. The arrival of this signal contribution is determined by the dynamics of that dominant saddle point that becomes exponentially negligible in comparison to the pole contribution. A detailed knowledge of the saddle point dynamics for a given dispersive material is then seen to be a critical ingredient for a detailed description of dispersive pulse propagation in that material, not just for the transient field behavior described by Eq. (20.19), but also for the steady-state behavior described in Eq. (20.20).

In a multiple resonance Lorentz model[56] dielectric the complex index of refraction is described by[46]

$$n(\omega) = \left(1 - \sum_{j=0}^{N} \frac{b_{2j}^2}{\omega^2 - \omega_{2j}^2 + 2i\delta_{2j}\omega} \right)^{1/2} , \qquad (20.21)$$

where ω_{2j} is the undamped resonance frequency, b_{2j} is the plasma frequency, and δ_{2j} the phenomenological damping constant for the $(2j)^{th}$ resonance line of the dielectric material. This causal model[52] provides an accurate description of both the normal and anomalous dispersion phenomena observed in homogeneous, isotropic, locally linear optical materials. The regions of anomalous dispersion approximately extend over each frequency domain $\left(\omega_{2j}, \omega_{2j+1}\right)$, where $\omega_{2j+1} \equiv \sqrt{\omega_{2j}^2 + b_{2j}^2}$. In this case the saddle point equation (20.14) has at least two sets of saddle points that are symmetrically situated about the imaginary axis. One pair of saddle points (the distant saddle points[11,12,43,46]) evolve in the high-frequency region $|\omega| \geq \omega_{2N+1}$ of the complex ω-plane above the uppermost absorption band of the material, while another pair of saddle points (the near saddle points[11,12,43,46]) evolve in the low-frequency region $|\omega| \leq \omega_0$ of the complex ω-plane below the lowermost absorption band of the dielectric. If the dielectric material is described by multiple resonance lines, then additional middle saddle points will appear in the region $|\omega| < \omega_{2N}$ below the uppermost absorption of the dielectric. The asymptotic description of the propagated pulse may then be expressed either in the form

$$A(z,t) \sim A_S(z,t) + A_m(z,t) + A_B(z,t) + A_c(z,t) \qquad (20.22)$$

as $\Delta z \to \infty$, or by an expression that is a superposition of expressions of the form given in Eq. (20.22).

Here $A_S(z,t)$ denotes the contribution from the distant saddle points with nonuniform asymptotic approximation given by Eq. (20.19) for $\theta > 1$ and is referred to as the first or Sommerfeld precursor. This nonuniform approximation breaks down at $\theta = 1$ when the distant saddle points are at infinity. The uniform asymptotic description[22,45,46] of the Sommerfeld precursor, uniformly valid in the space-time parameter $\theta = ct/\Delta z$ for all $\theta \geq 1$, must then be used in place of Eq. (20.19) for the initial pulse evolution. The instantaneous angular oscillation frequency of the Sommerfeld precursor is approximately given by the real part of the distant saddle point location[43,46] in the right-half of the complex ω-plane. The Sommerfeld precursor then describes the signal front which arrives at $\theta = 1$ with infinite oscillation frequency (but zero amplitude for a finite energy input pulse) and consequently propagates at the speed of light c in vacuum. As θ increases away from unity, the amplitude of the Sommerfeld precursor rapidly increases to a maximum value and then decreases monotonically for all larger θ while the instantaneous

20.5. Accuracy of the Group Velocity Description of Ultrashort Pulse Dynamics

The accuracy of the group velocity approximation of ultrashort pulse dispersion is now considered in order to establish the space-time domain over which this approximate description is valid. A double resonance Lorentz model of a fluoride-type glass with infrared ($\omega_0 = 1.74\times10^{14}\, r/s$, $b_0 = 1.22\times10^{14}\, r/s$, $\delta_0 = 4.96\times10^{13}\, r/s$) and near ultraviolet ($\omega_2 = 9.145\times10^{15}\, r/s$, $b_2 = 6.72\times10^{15}\, r/s$, $\delta_2 = 1.434\times10^{15}\, r/s$) resonance lines is considered with complex index of refraction given by Eq. (20.21) with $N = 2$. The angular frequency dispersion of the real and imaginary parts of the complex wavenumber $\tilde{k}(\omega) = (\omega/c)n(\omega)$ for this double resonance Lorentz model dielectric is illustrated in Figure 1. The upper and lower solid curves in each part of the figure describe the exact frequency dependence of $\beta(\omega) \equiv \Re\{\tilde{k}(\omega)\}$ and $\alpha(\omega) \equiv \Im\{\tilde{k}(\omega)\}$, respectively, while the dashed red curves describe the cubic dispersion approximation when (a) $\omega_c = \omega_{\min} = 1.615\times10^{15}\, r/s$ and (b) $\omega_c = 0.87\omega_2 = 8.0\times10^{15}\, r/s$. The cubic dispersion approximation is seen to provide a reasonably accurate estimate of the local frequency dispersion of the propagation factor $\beta(\omega)$ about the carrier frequency within the passband where the dispersion is normal when $\omega_c = \omega_{\min}$, but the accuracy of this approximation is seen to decrease[48,49] as ω_c is shifted toward either absorption band where the dispersion becomes anomalous. The inclusion of higher-order terms in the Taylor series approximation of the complex wavenumber only serves to further decrease its accuracy in a global sense[48,49]. The cubic dispersion approximation of the attenuation coefficient is not as accurate as that for the propagation factor making the necessity of the approximation $\alpha(\omega) \approx \alpha(\omega_c)$ used in the group velocity description all the more important.

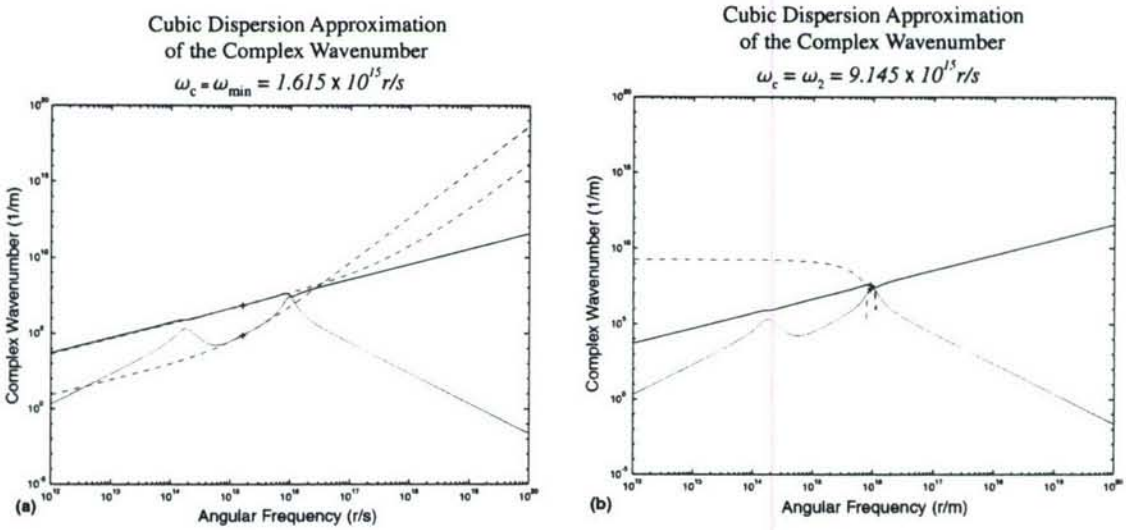

Figure 1. Angular frequency dependence of the real (upper solid curves) and imaginary (lower solid curves) parts of the complex wavenumber for a double resonance Lorentz model of a fluoride-type glass with infrared and near ultraviolet resonance lines. In part (a) the dashed curves describe the cubic dispersion approximation about the minimum dispersion point in the passband between the absorption bands and in part (b) they describe that approximation about the upper resonance frequency.

Because of its central importance in ultrashort optical pulse technology, a unit amplitude gaussian envelope pulse $f(t) = u(t)\sin(\omega_c t + \pi/2)$ is considered, where

superluminal and negative. Part (a) of the figure illustrates the approximate group velocity and actual pulses at one absorption depth $\Delta z = z_d$ in the medium, where $z_d = \alpha^{-1}(\omega_c)$; the actual pulse is clearly not travelling at a rate given by the classical group velocity $v_g(\omega_c) = 1/\beta'(\omega_c)$. Part (b) of the figure illustrates the actual and approximate pulses when the approximate group velocity pulse (dashed curve) has been temporally shifted such that its peak amplitude point is coincident with that for the actual pulse (solid curve). The error between these two pulses is then computed in two different ways. The first error measure (error1) is given by the integral of the square of the difference between the two aligned pulses. This error then measures both shape and energy differences. The second error measure (error2) is obtained by first renormalizing both pulses by the square root of their respective pulse energies and then taking the integral of the square of their differences. This error then measures the shape difference between the two aligned pulses at a given fixed propagation distance.

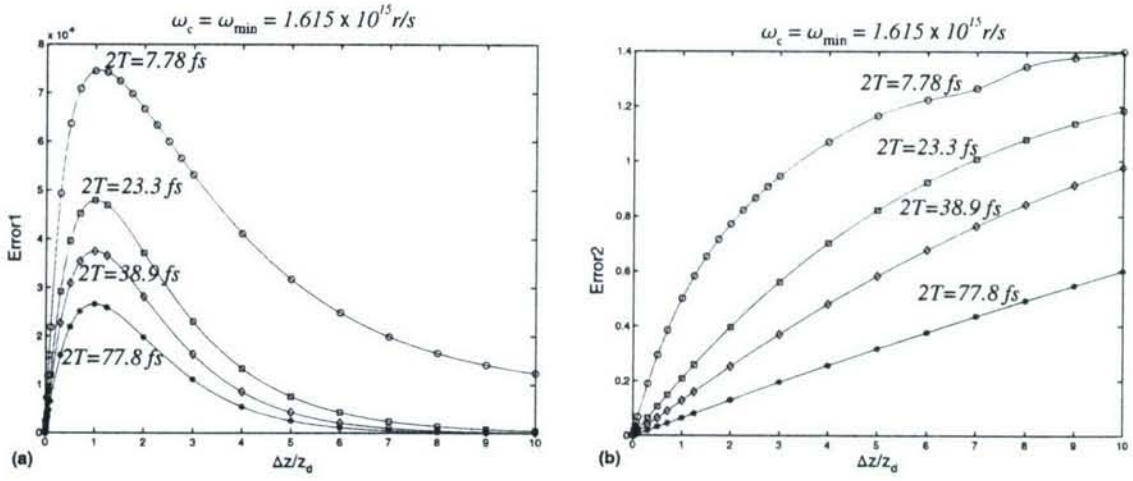

Figure 3. Error resulting from the group velocity description of the propagated gaussian envelope pulse with a cubic dispersion approximation of the propagation factor $\beta(\omega)$ in a double resonance Lorentz model dielectric as function of the relative penetration depth $\Delta z/z_d$ when the input pulse carrier frequency ω_c is equal to the angular frequency ω_{min} at the minimum dispersion point in the passband between the two absorption bands for different values of the input pulse width $2T$.

The numerical results for these two error measures are depicted in Figure 3 as a function of the relative propagation distance $\Delta z/z_d$ when the input pulse carrier angular frequency ω_c is set equal to the angular frequency ω_{min} at the minimum dispersion point in the passband between the two absorption bands of the double resonance Lorentz model dielectric. The results are presented for four different values of the input gaussian envelope pulse width $2T$. The results clearly show that, as expected, the error decreases with increasing initial pulse width at any fixed value of the propagation distance. The first error measure (error1) is seen in part (a) of the figure to initially increase with increasing propagation distance, reaching a peak value at approximately one absorption depth ($\Delta z/z_d \sim 1$), and then decreasing to zero as the relative propagation distance $\Delta z/z_d$ increases above unity. This behavior is due to the fact that the group velocity approximate pulse amplitude decays exponentially with penetration distance at a faster rate than does the actual ultrashort pulse so that the observed monotonic decrease in error with increasing propagation distance $\Delta z/z_d > 1$ primarily describes the slow, nonexponential amplitude decay with propagation distance of the actual pulse in the lossy dielectric. This difference between the

20.6. The Question of Superluminal Pulse Velocities

A number of velocity measures have been introduced for the purpose of describing the rate at which some particular feature of a pulse travels through a dispersive material. The most important of these are the phase[3], group[1-4,30-32], energy[38,41], signal[5-12,18,43-47], and centroid[61-65] velocities. Each of these velocity measures in free space equals the velocity of light c in vacuum, but they are in general different in a causally dispersive material such as that described by the Lorentz model.

The phase velocity $v_p(\omega) \equiv \omega/\beta(\omega)$ describes the rate at which the co-phasal surfaces propagate through the dispersive medium[3] [cf. Eqs. (20.9)-(20.10)]. Since the phase of a spatially coherent optical field can only be measured indirectly[66], this velocity measure does not have any separate, measurable physical meaning in spite of the fact that it plays a central role in the mathematical description of pulse dispersion, as described by Eq. (20.1). In particular, the phase velocity of a pulse is superluminal [i.e. $v_p(\omega_c) > c$] when the input pulse carrier frequency ω_c is above the uppermost absorption band of a Lorentz model dielectric, as illustrated in Fig. 5(a) for a single resonance Lorentz model dielectric when $\omega_c > \omega_1$. For an ultrashort pulse with above resonance carrier frequency whose temporal energy centroid is moving subluminally, the phase velocity is then seen to describe the motion of a space-time point where there is negligible pulse energy.

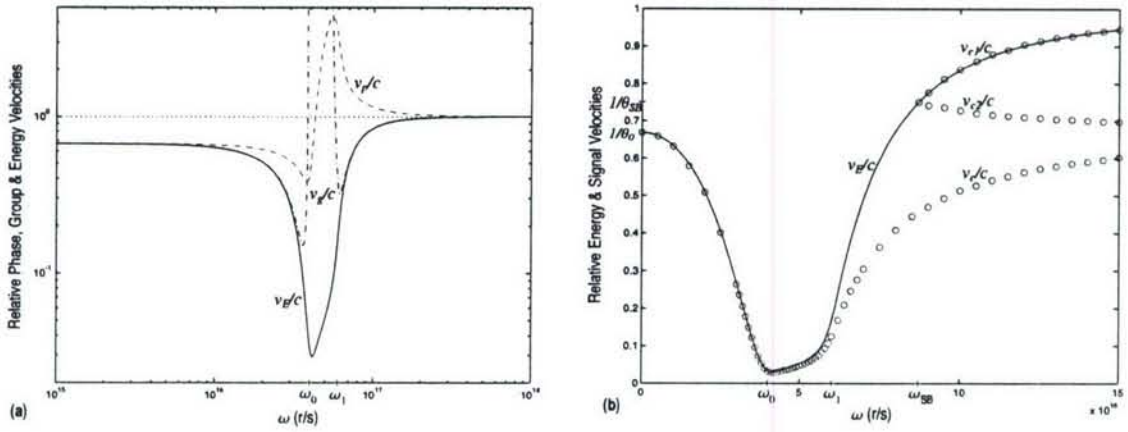

Figure 5. Frequency dependence of (a) the relative phase velocity (dashed curve), group velocity (dash-dot curve) and energy velocity (solid curve) and (b) the relative energy velocity (solid curve) and signal velocity (open circles) in a single resonance Lorentz model dielectric.

The group velocity $v_g(\omega) \equiv \left(\partial\beta(\omega)/\partial\omega\right)^{-1}$ describes the rate at which the envelope of a group of waves travels through the dispersive medium[1-4] [cf. Eqs. (20.9) and (20.11)]. As described by Rayleigh[3], a group of waves is defined as moving beats following each other in a regular pattern as, for example, that obtained from the coherent superposition of two monochromatic waves with slightly different amplitudes and frequencies. Although the group velocity does indeed describe the beat velocity of such an infinite wave group, its extension to the description of the velocity of an ultrashort pulse in a causally dispersive medium is invalid. This is readily evident in Fig. 2(a) where the group velocity approximate pulse is seen to be moving at a faster rate than is the actual pulse. This example illustrates the extreme dispersion case when $\omega_c = \omega_2$. The group velocity value $v_g(\omega_c)$ is then seen to be a poor measure of the actual pulse velocity when the material loss is not negligible, although it can describe the initial pulse evolution when the material loss is near

For the numerical gaussian pulse example illustrated in Fig. 2, the peak amplitude point of the actual pulse is moving with the average velocity $v_{peak} \cong 0.91c$ and the peak amplitude point of the group velocity approximate pulse is moving with the average velocity $v_{peak}^{app} \cong -0.30c$, while the phase velocity is given by $v_p(\omega_c) \cong 0.82c$, the group velocity is given by $v_g(\omega_c) \cong -0.41c$, and the energy velocity is given by $v_E(\omega_c) \cong 0.18c$ at the input pulse carrier angular frequency $\omega_c = \omega_2 = 9.145 \times 10^{15}\, r/s$. The peak amplitude values reported here are "time-of-flight" values that result from numerical measurements of the initial and final pulse positions. This average peak amplitude velocity measure changes as the propagation distance into the dispersive dielectric increases, as does the instantaneous peak amplitude velocity. The instantaneous peak amplitude velocity of an ultrashort gaussian pulse has been shown[59,60] to evolve with increasing propagation distance along the group velocity curve toward the energy velocity curve as the instantaneous oscillation frequency at the peak amplitude point shifts away from the region of anomalous dispersion and into the normal dispersion region either above or below that absorption band. It is then not surprising that the numerical velocity values given above are all significantly different as each describes a different feature of the pulse that may only be valid either in the limit of vanishingly small propagation distance (the group velocity) or else in the large propagation distance asymptotic limit (the energy velocity).

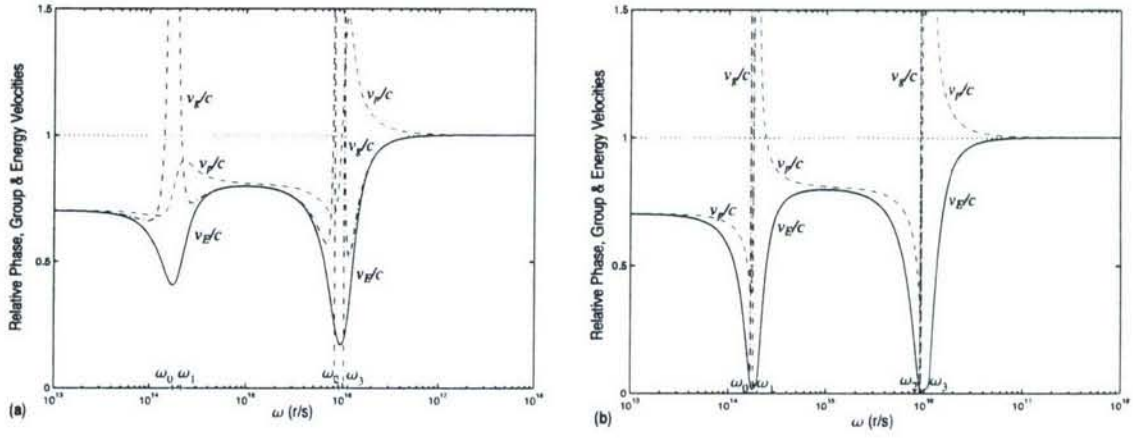

Figure 6. Frequency dependence of the relative phase velocity (dashed curves), group velocity (dash-dot curves) and energy velocity (solid curves) for (a) the double resonace Lorentz model dielectric considered in Fig. 1 and (b) the same double resonance Lorentz model dielectric when each of the phenomenological damping constants have been reduced by a factor of ten.

It is clear that a more physically meaningful pulse velocity measure needs to be considered in order to accurately describe the complicated pulse evolution that occurs in ultrashort dispersive pulse dynamics. One possible measure is given by the pulse centrovelocity[61]

$$v_{CE} \equiv \left| \nabla \left(\int_{-\infty}^{\infty} tE^2(\boldsymbol{r},t)dt \Big/ \int_{-\infty}^{\infty} E^2(\boldsymbol{r},t)dt \right) \right|^{-1}, \tag{20.26}$$

which describes the temporal center of gravity of the pulse intensity. A more appropriate velocity measure would track the temporal centroid of the Poynting vector of the pulse. This pulse centroid velocity of the Poynting vector was first introduced by Lisak[62] in 1976. Recent descriptions[63-65] of its properties have established its efficacy in describing the evolution of the

distances to its asymptotic behavior for large propagation distances. The minimum point in this dip occurs at a propagation distance whose value increases with increasing initial pulse width while the minimum value decreases with increasing initial pulse width. At the leading edge of each dip when the centrovelocity rapidly decreases, the pulse begins to separate into a pair of middle and Brillouin precursors and the temporal pulse centroid is found to occur at a space-time point between these two pulse components where the pulse energy is minimal. Finally, notice that the centrovelocity for a gaussian pulse is subluminal and nonnegative (i.e., $0 \le v_{CI} \le c$) for all propagation distances at this input carrier frequency.

In Fig. 7(b) the input pulse carrier frequency is set equal to the upper resonance frequency ω_2 of the double resonance Lorentz model dielectric where the dispersion is anomalous. The classical group velocity limit $v_g(\omega_c) \cong -0.4076c$ is again approached at a sufficiently small propagation distance in the limit as the initial pulse width increases and the initial pulse spectrum narrows about the carrier frequency ω_c, but at a much slower rate than that obtained at the minimum dispersion point. However, notice that if the initial pulse width is sufficiently small (as it is for the $1.37fs$ pulse case), then the initial pulse spectrum is extremely ultrawideband such that the classical group velocity limit is not obtained as $\Delta z \to 0$ and the centrovelocity remains positive for all propagation distances $\Delta z \ge 0$. In the opposite limit as $\Delta z/z_d \to \infty$ the centroid velocity is again found to approach the velocity $v_B = c/n(0)$ that the peak amplitude point in the Brillouin precursor travels at through the dispersive material. For a sufficiently long initial pulse width, the transition of the ultrawideband pulse centroid velocity between these two limits is marked by a rapid decrease in centrovelocity to $-\infty$ and then from $+\infty$ to subluminal values before approaching the asymptotic limit $v_B = c/n(0)$ set by the peak amplitude point of the Brillouin precursor. The discontinuous jump in the centrovelocity from $-\infty$ to $+\infty$ is found to occur at a relative propagation distance whose value increases with increasing pulse width provided that the initial pulse spectrum is ultrawideband.

In spite of the fact that the instantaneous centrovelocity of the pulse Poynting vector can take on both negative and superluminal values for sufficiently small relative propagation distances, the pulse itself is found to only undergo a slight change in shape. There isn't any superluminal movement of the pulse when the instantaneous pulse centrovelocity is superluminal, nor is there any retrogression in position when the pulse centrovelocity is negative. Sommerfeld's theorem firmly establishes that electromagnetic field energy cannot move forward of any space-time point in the pulse at a superluminal rate. Finally, notice that this seemingly nonphysical behavior only occurs in the immature dispersion regime ($0 \le \Delta z < z_c$) where the group velocity approximation applies in the limit as $\Delta z \to 0$.

20.7. Conclusions

The analysis and numerical results presented in this paper have established the following results: (1) The group velocity approximation is valid only in the immature dispersion regime $0 \le \Delta z < z_c$, its accuracy increasing as $\Delta z \to 0$. The asymptotic description is valid in the mature dispersion regime $\Delta z > z_c$, its accuracy increasing in the sense of Poincaré[17] as $\Delta z \to \infty$. The critical distance z_c depends upon the input pulse type and initial pulse length, as well as upon the input pulse carrier frequency for a given dispersive material. (2) The instantaneous centroid velocity of the pulse Poynting vector is a convenient, albeit sometimes misleading, measure of the pulse evolution in a dispersive medium for input gaussian envelope pulses. Although this velocity measure can take on both negative and superluminal values for relative propagation distances in

18. H. Baerwald, "Über die Fortpflanzung von Signalen in dispergierenden Systemen,"*Ann. Physik* **7**, 731-760 (1930).
19. J. A. Stratton, *Electromagnetic Theory*, §5.18, McGraw-Hill, (1941).
20. N. S. Shiren, "Measurement of signal velocity in a region of resonant absorption by ultrasonic paramagnetic resonance," *Phys. Rev.* **128**, 2103-2112 (1962).
21. T. A. Weber and D. B. Trizna, "Wave propagation in a dispersive and emissive medium," *Phys. Rev.* **144**, 277-282 (1966).
22. R. A. Handelsman and N. Bleistein, "Uniform asymptotic expansions of integrals that arise in the analysis of precursors," *Arch. Rational Mech. Analysis* **35**. 267-283 (1969).
23. P. Pleshko and I. Palócz, "Experimental observation of Sommerfeld and Brillouin precursors in the microwave domain," *Phys. Rev. Lett.* 22, 1201-1204 (1969).
24. C. Eckart, "The approximate solution of one-dimensional wave equations," *Rev. Modern Physics* 20, 399-417 (1948).
25. R. M. Lewis, "Asymptotic theory of wave propagation," *Arch. Rational Mech. Analysis* **20**, 191-250 (1065).
26. R. M. Lewis, "Asymptotic theory of transients," in *Electromagnetic Wave Theory*, J. Brown, ed., pp. 845-869, Pergamon Press (1967).
27. L. B. Felsen, "Rays, dispersion surfaces and their uses for radiation and diffraction problems," *SIAM Review* **12**, 424-448 (1970).
28. K. A. Connor and L. B. Felsen, "Complex-space-time rays and their application to pulse propagation in lossy dispersive media," *Proc. IEEE* **62**, 1586-1598 (1974).
29. D. Censor, "Fermat's principle and real space-time rays in absorbing media," *J. Phys. A* **10**, 1781-1790 (1977).
30. M. A. Biot, "General theorems on the equivalence of group velocity and energy transport," *Phys. Rev.* **105**, 1129-1137 (1957).
31. G. B. Whitham, "Group velocity and energy propagation for three-dimensional waves," *Comm. Pure and Applied Math.* **XIV**, 675-691 (1961).
32. M. J. Lighthill, "Group velocity," *J. Inst. Maths. Applics.* **1**, 1-28 (1964).
33. M. Born and E. Wolf, *Principles of Optics*, chapter 10, Pergamon Press (1959).
34. J. Jones, "On the propagation of a pulse through a dispersive medium," *Am. J. Phys.* **42**, 43-46 (1974).
35. D. G. Anderson and J. I. H. Askne, "Wave packets in strongly dispersive media," *Proc. IEEE* **62**, 1518-1523 (1974).
36. D. Anderson, J. Askne and M. Lisak, "Wave packets in an absorptive and strongly dispersive medium," *Phys. Rev. A* **12**, 1546-1552 (1975).
37. E. O. Schulz-DuBois, "Energy transport velocity of electromagnetic propagation in dispersive media," *Proc. IEEE* **57**, 1748-1757 (1969).
38. R. Loudon, "The propagation of electromagnetic energy through an absorbing dielectric," *J. Phys. A* **3**, 233-245 (1970).
39. G. C. Sherman and K. E. Oughstun, "Description of pulse dynamics in Lorentz media in terms of the energy velocity and attenuation of time-harmonic waves," *Phys. Rev. Lett.* **47**, 1451-1454 (1981).
40. G. C. Sherman and K. E. Oughstun, "Energy velocity description of pulse propagation in absorbing, dispersive dielectrics," *J. Opt. Soc. Am. B* **12**, 229-247 (1995).
41. K. E. Oughstun and S. Shen, "The velocity of energy transport for a time-harmonic field in a multiple resonance Lorentz medium," *J. Opt. Soc. Am. B* **5**, 2395-2398 (1988).
42. D. Trizna and T. Weber, "Brillouin revisited: Signal velocity definition for pulse propagation in a medium with resonant anomalous dispersion," *Radio Sci.* **17**, 1169-1180 (1982).
43. K. E. Oughstun and G. C. Sherman, "Propagation of electromagnetic pulses in a linear dispersive medium with absorption (the Lorentz medium)," *J. Opt. Soc. Am. B* **5**, 817-849 (1988).

Magnetic field contribution to the Lorentz model

Kurt E. Oughstun

College of Engineering and Mathematical Sciences, University of Vermont, Burlington, Vermont 05405-0156

Richard A. Albanese

Information Operations and Special Projects Division, U. S. Air Force Research Laboratory, Brooks City-Base, Texas 78235

Received November 10, 2005; accepted December 8, 2005; posted January 24, 2006 (Doc. ID 65838)

The classical Lorentz model of dielectric dispersion is based on the microscopic Lorentz force relation and Newton's second law of motion for an ensemble of harmonically bound electrons. The magnetic field contribution in the Lorentz force relation is neglected because it is typically small in comparison with the electric field contribution. Inclusion of this term leads to a microscopic polarization density that contains both perpendicular and parallel components relative to the plane wave propagation vector. The modified parallel and perpendicular polarizabilities are both nonlinear in the local electric field strength. © 2006 Optical Society of America

OCIS codes: 260.2030, 190.4400, 160.4760, 160.4330.

1. INTRODUCTION

The Lorentz model[1–3] of resonant dispersion phenomena in dielectric materials is a classical model of central importance in optics[4,5] as well as in the broader discipline of electromagnetics.[6] It is a causal model[6,7] that describes both normal and anomalous dispersion phenomena from the infrared through the optical regions of the electromagnetic spectrum. This model is based on the microscopic Lorentz force relation

$$\mathbf{f}(\mathbf{r},t) = \rho(\mathbf{r},t)\mathbf{e}(\mathbf{r},t) + \frac{1}{\|c\|}\mathbf{j}(\mathbf{r},t)\times\mathbf{b}(\mathbf{r},t), \tag{1}$$

where $\rho(\mathbf{r},t)$ is the microscopic change density and $\mathbf{j}(\mathbf{r},t) = \rho(\mathbf{r},t)\mathrm{d}\mathbf{r}/\mathrm{d}t$ the microscopic current density of the charged particle at the space–time point $(\mathbf{r},t)$ and where $\mathbf{f}(\mathbf{r},t)$ is the microscopic force density exerted on the charged particle by the electromagnetic field with microscopic electric intensity vector $\mathbf{e}(\mathbf{r},t)$ and magnetic induction vector $\mathbf{b}(\mathbf{r},t)$. The quantity $*$ appearing in the double brackets $\|*\|$ in any equation here is used as a conversion factor between cgs and MKS units.[6,8] If that factor is included in that equation, then the equation is in cgs units, while if the factor is omitted from that equation, then it is in MKS units. If no such factor appears in a given equation, then that equation is correct in either system of units.

The magnetic field contribution appearing on the right-hand side of Eq. (1) is typically assumed to be negligible in comparison with the electric field contribution for sufficiently small field strengths and values of the relative velocity v/c of the charged particle, where $v = |\mathrm{d}\mathbf{r}/\mathrm{d}t|$. This assumption then leads to the classical Lorentz theory of dielectric dispersion in which electric field effects alone are considered. The question then remains as to what effects are introduced by the inclusion of the magnetic field contribution in the Lorentz theory. The solution of this important problem has been partially addressed[9–11] for the special case of a chiral molecule, where it has been shown[11] that the magnitude of the magnetic response of the induced second-order optical activity can be comparable to the magnitude of the electric response alone. However, as we have been unable to find any previously published general solution of this problem, it is addressed in this paper.

2. MODIFIED LORENTZ MODEL OF DIELECTRIC DISPERSION

With the complete Lorentz force relation given in Eq. (1) as the driving force, the equation of motion of a harmonically bound electron is given by

$$\frac{\mathrm{d}^2\mathbf{r}_j}{\mathrm{d}t^2} + 2\delta_j\frac{\mathrm{d}\mathbf{r}_j}{\mathrm{d}t} + \omega_j^2\mathbf{r}_j = -\frac{q_e}{m}\left(\mathbf{E}_{eff}(\mathbf{r},t) + \frac{1}{\|c\|}\frac{\mathrm{d}\mathbf{r}_j}{\mathrm{d}t}\times\mathbf{B}_{eff}(\mathbf{r},t)\right), \tag{2}$$

where $\mathbf{E}_{eff}(\mathbf{r},t)$ is the effective local electric field intensity and $\mathbf{B}_{eff}(\mathbf{r},t)$ is the effective local magnetic induction field at the space–time point $(\mathbf{r},t)$ and where $\mathbf{r}_j = \mathbf{r}_j(\mathbf{r},t)$ describes the displacement of the electron from its equilibrium position. Here q_e denotes the magnitude of the charge and m the mass of the harmonically bound electron with undamped resonance frequency ω_j and phenomenological damping constant δ_j. The temporal Fourier integral representation of the electric and magnetic field vectors of the effective local plane electromagnetic wave is given by[8]

$$\tilde{\mathbf{E}}_{eff}(\mathbf{r},\omega) = \int_{-\infty}^{\infty}\mathbf{E}_{eff}(\mathbf{r},t)e^{i\omega t}\mathrm{d}t, \tag{3}$$

1084-7529/06/071751-6/$15.00

when magnetic field effects are neglected, and

$$\alpha_{j\parallel}(\omega,\tilde{E}_{eff}) \equiv i\frac{(q_e^3/m^2)\tilde{E}_{eff}^2}{(\omega^2-\omega_j^2+2i\delta_j\omega)^2-(q_e/mc)^2\tilde{E}_{eff}^2\omega^2} \quad (18)$$

is defined here as the parallel component of the atomic polarizability, where $\alpha_{j\parallel}(\omega,0)=0$.

3. CRITICAL FIELD STRENGTH

The atomic polarizability is then seen to be nonlinear in the local electric field strength when magnetic field effects are included. The nonlinear term $\alpha_{j\perp}^{(2)}(\omega,\tilde{E}_{eff})$ appearing in Eq. (17) will be negligible in comparison with the linear term $\alpha_{j\perp}^{(0)}(\omega)$ when the local electric field strength is sufficiently smaller than the critical field strength $E_{crit}=E_{crit}(\omega)$ defined by the condition

$$\left|\frac{(q_e/mc)^2\tilde{E}_{crit}^2\omega^2}{(\omega^2-\omega_j^2+2i\delta_j\omega)^2-(q_e/mc)^2\tilde{E}_{crit}^2\omega^2}\right| \equiv 1,$$

with solution

$$E_{crit}(\omega) = \frac{mc}{\sqrt{2}q_e}\frac{(\omega^2-\omega_j^2)^2+4\delta_j^2\omega^2}{\omega[(\omega^2-\omega_j^2)^2-4\delta_j^2\omega^2]^{1/2}}. \quad (19)$$

When $|\tilde{E}_{eff}| \ll E_{crit}$, the linear term in Eq. (17) dominates the nonlinear term so that $\alpha_{j\perp}(\omega,\tilde{E}_{eff}) \simeq \alpha_{j\perp}^{(0)}(\omega)$. Notice that this critical electric field strength depends on the value of the applied angular frequency ω of the electromagnetic wave field. Furthermore, notice that this critical field strength in undefined in the angular frequency band $\omega \in [\omega_j^-,\omega_j^+]$, where

$$\omega_j^{\pm} \equiv (\omega_j^2+2\delta_j^2 \pm 2\delta_j\sqrt{\omega_j^2+\delta_j^2})^{1/2} \quad (20)$$

for each resonance feature j, where $\omega_j \in [\omega_j^-,\omega_j^+]$. Finally, a rough estimate of the minimum value for this critical field strength is seen to be given by

$$(E_{crit})_{min} \approx \frac{mc}{\sqrt{2}q_e}\omega_j = \frac{\hbar\omega_j}{\sqrt{8}\mu_B} \quad (21)$$

for each resonance feature, where $\mu_B \equiv q_e\hbar/2mc$ is the Bohr magneton. The quantity $\hbar\omega_j$ is recognized as the energy level state of the harmonically bound electron.

4. NUMERICAL EXAMPLE

Consider a single resonance Lorentz model dielectric ($j=0$) with material parameters representative of the near-infrared line in triply distilled water at 25 °C, where $\omega_0=6.19\times10^{14}$ r/s and $\delta_0=2.86\times10^{13}$ r/s. The angular frequency dependence of the real and imaginary parts of the linear atomic polarizability $\alpha_{j\perp}^{(0)} \equiv \alpha_j(\omega)$ for this single resonance line is presented in Fig. 1, and the angular frequency dependence of the critical field strength described by Eq. (19) is illustrated in Fig. 2, where $\omega_0^- \simeq 5.91\times10^{14}$ r/s and $\omega_0^+ \simeq 6.48\times10^{14}$ r/s. The minimum critical electric field strength $(E_{crit})_{min} \simeq 1.38\times10^{11}$ V/m is seen to occur at the two points just below and above the frequency band $[\omega_0^-,\omega_0^+]$ where the critical field strength is undefined; the estimate given by Eq. (21) yields an approximate value of 7.5×10^{11} V/m. Notice that $E_{crit}\to\infty$ at both of the near-resonance values $\omega_0^{\pm}$ as well as when either $\omega\to0$ or $\omega\to\infty$. Notice also that since megavolt per meter electric field strengths are produced by ultrashort pulsed terawatt laser systems, the minimum critical field strength for this example is at least five orders of magnitude greater than that which is currently available.

The angular frequency dependence of the relative correction factor $\alpha_{j\perp}^{(2)}(\omega,\tilde{E}_{eff})/\alpha_{j\perp}^{(0)}(\omega)$ for the perpendicular atomic polarizability given in Eq. (17) is illustrated in Fig. 3 for the near-infrared resonance line of triply distilled water for several values of the relative local electric field intensity about unity. Notice that this correction factor reaches its peak value at the resonance frequency ω_0 when $|\tilde{E}_{eff}/(E_{crit})_{min}|<1$ and that this peak value bifurcates into a pair of symmetric peaks about this resonance frequency when $|\tilde{E}_{eff}/(E_{crit})_{min}|>1$, a local minimum now

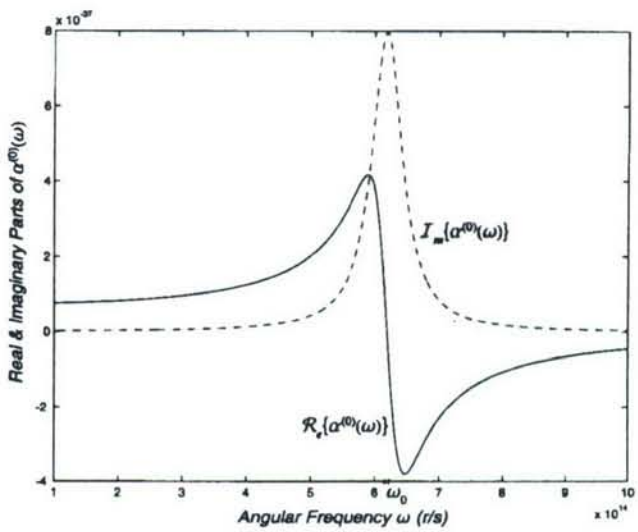

Fig. 1. Real (solid curve) and imaginary (dashed curve) parts of the linear atomic polarizability for the near-infrared resonance line in water.

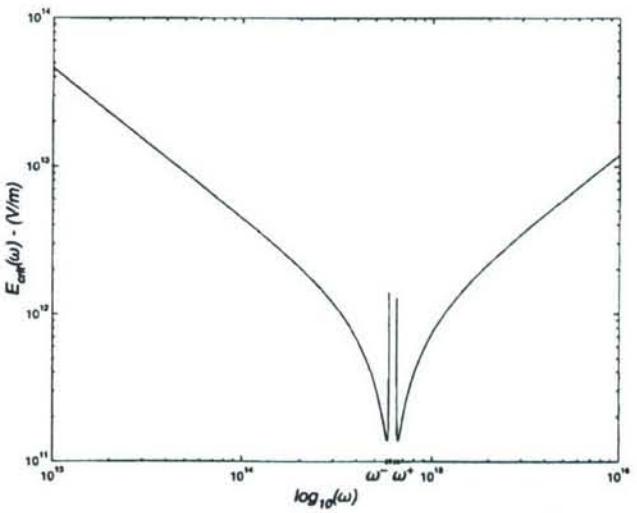

Fig. 2. Angular frequency dependence of the critical local electric field strength (in volts per meter) for the near-infrared resonance line in water.

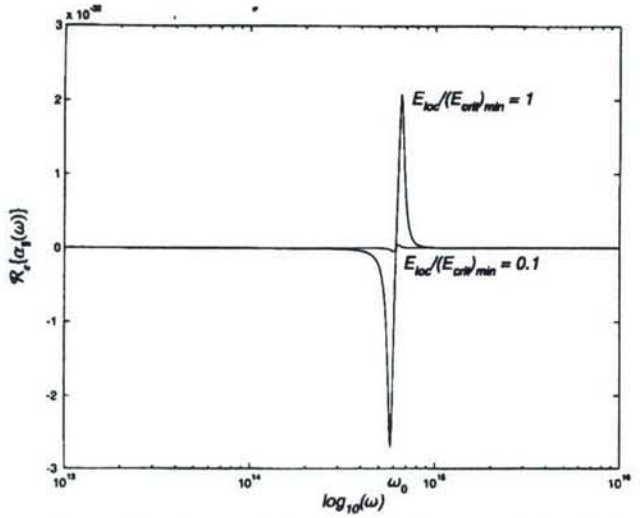

Fig. 6. Angular frequency dependence of the real part of the longitudinal atomic polarizability for critical and subcritical values of the local electric field strength.

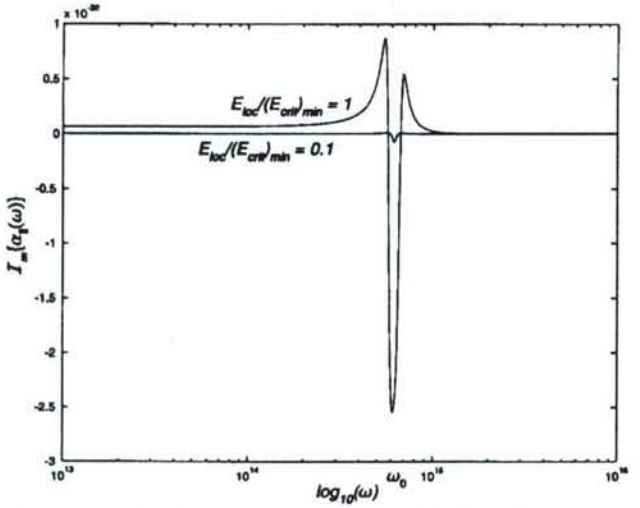

Fig. 7. Angular frequency dependence of the imaginary part of the longitudinal atomic polarizability for critical and subcritical values of the local electric field strength.

$$\omega_+ \approx \frac{\hbar\omega_j^2}{2\mu_B\tilde{E}_{eff}} + \frac{2\mu_B}{\hbar}\tilde{E}_{eff}, \tag{24}$$

$$\omega_- \approx \frac{\hbar\omega_j^2}{2\mu_B\tilde{E}_{eff}}, \tag{25}$$

are obtained.

Similar results are obtained for the frequency dependence of the nonlinear character of the parallel atomic polarizability given in Eq. (18). Although this parallel component of the atomic polarizability vanishes as $\tilde{E}_{eff} \to 0$, it can exceed the strength of the transverse component of the atomic polarizability when $\tilde{E}_{eff}$ exceeds the minimum critical field strength. The frequency dependence of the real part of the longitudinal (parallel) component is presented in Fig. 6 and the imaginary part in Fig. 7 for two values of the local electric field strength. Both the real and the imaginary parts are seen to exhibit a pronounced resonance about the undamped resonance frequency ω_0 when the local electric field strength is equal to or less than the minimum critical field strength $(E_{crit})_{min}$ given in Eq. (21). However, as the local field strength exceeds this minimum critical value, this single resonance peak is found to split into a pair of resonance structures, one downshifted and the other uphifted in angular frequency from the characteristic resonance frequency ω_0 of the Lorentz model dielectric.

5. DISCUSSION

The results presented here show the precise manner in which the magnetic field influences the atomic polarizability in the Lorentz model of resonance polarization. Inclusion of the magnetic field in the Lorentz force relation results in a microscopic polarization density that contains both perpendicular and parallel components relative to the plane wave propagation vector of the local driving field that are both nonlinear in the local electrical field strength. This nonlinearity becomes significant when the local applied electric field strength exceeds a minimum critical field strength whose value increases linearly with the resonance frequency. Numerical calculations show that these nonlinear terms are entirely negligible for effective field strengths that are typically less than $\sim 10^{12}$ V/m and that they begin to have a significant contribution for field strengths that are typically greater than $\sim 10^{15}$ V/m for a highly absorptive material. Fortunately, this critical field strength is at least five orders of magnitude greater than that which is currently available in ultrashort pulsed terawatt laser systems. Although this magnetic field effect is negligible in most practical situations, it has been shown to be significant in materials exhibiting chirality,[9–11] and it may also become important for artificial materials. Nevertheless, seemingly excessive electric field strengths commonly occur in nature; for example, it is estimated[12] that the critical field strength for the alignment of water molecules for crystallization into polar ice crystals is greater than 10^9 V/m.

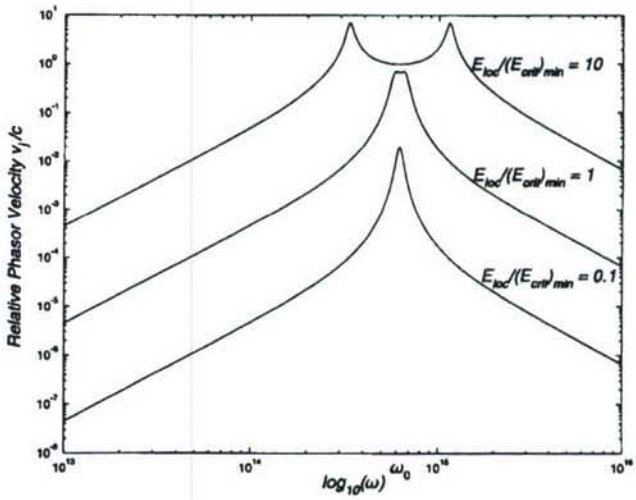

Fig. 8. Angular frequency dependence of the relative phasor velocity magnitude of the harmonically bound electron in the Lorentz model.

SIAM REVIEW
Vol. 49, No. 4, pp. 000–000

Uniform Asymptotics Applied to Ultrawideband Pulse Propagation*

Natalie A. Cartwright†
Kurt E. Oughstun†

Abstract. A canonical problem of central importance in the theory of ultrawideband pulse propagation through temporally dispersive, absorptive materials is the propagation of a Heaviside step-function signal through a medium that exhibits anomalous dispersion. This problem is rich in the use of asymptotic theory. Sommerfeld and Brillouin provided the first (qualitatively accurate but quantitatively inaccurate) closed-form approximations of the dynamic evolution of this waveform through a single-resonance Lorentz model dielectric based upon Debye's method of steepest descent. An improved approximation has since been provided by Oughstun and Sherman using modern, uniform asymptotic methods that rely upon the saddle-point method. An accurate, uniform asymptotic approximation describing the dynamical evolution of the unit step-function modulated sine wave signal through a single-resonance Lorentz model dielectric is presented here based upon their work. This refined asymptotic description results in a continuous evolution of the propagated field for all space-time points.

Key words. asymptotic methods, dispersive attenuative wave propagation

AMS subject classifications. 78M35, 78A40, 30E15

DOI. 10.1137/050635833

1. Introduction.

Asymptotic analysis is widely used in the study of pulse propagation in electromagnetics, optics, and acoustics. Typical applications include the study of the propagated pulse evolution as either the propagation distance or the wavelength becomes either large or small. Here, we study two-dimensional (space and time) electromagnetic pulse propagation through an unbounded dielectric material and show that many facets of uniform asymptotic theory are drawn upon in order to provide a continuous asymptotic approximation to the propagated pulse.

Consider a linearly polarized plane-wave electromagnetic pulse traveling in the positive z-direction. The material through which the pulse travels is a linear dielectric whose relative magnetic permeability μ is unity and whose relative dielectric permittivity $\epsilon(\omega)$ is given by the single-resonance Lorentz [18] dielectric model so that the complex index of refraction $n(\omega) = \sqrt{\mu\epsilon}$ is given by

$$n(\omega) = \left(1 - \frac{\omega_p^2}{\omega^2 - \omega_0^2 + 2i\delta\omega}\right)^{1/2}. \tag{1.1}$$

*Received by the editors July 12, 2005; accepted for publication (in revised form) July 28, 2006; published electronically November 1, 2007. This work was supported by the Air Force Office of Scientific Research under grant 9550-04-1-0447.
http://www.siam.org/journals/sirev/49-4/63583.html

†College of Engineering and Mathematics, University of Vermont, Burlington, VT 05401 (ncartwri@cems.uvm.edu). Questions, comments, or corrections to this document may be directed to this e-mail address.

Brillouin found two sets of saddle points: the contributions from the *distant saddle points* are responsible for the first forerunner, which had been evaluated for small $\theta \geq 1$ by Sommerfeld; the contributions from the *near saddle points* give rise to a second forerunner which begins after the arrival of the first forerunner. Brillouin also identified the main signal, characterized by its harmonic oscillation at the carrier frequency ω_c of the input pulse, which arrives after the second forerunner. Sommerfeld and Brillouin mistakenly concluded that both forerunners are of negligible amplitude in comparison to the amplitude of the main signal.

Although Sommerfeld and Brillouin correctly predicted the existence of the first and second forerunners, they did not accurately describe their behavior. It wasn't until 1975 when Oughstun and Sherman [25, 26] examined Sommerfeld's and Brillouin's seminal works that an accurate description of these two forerunners (now known as the Sommerfeld and Brillouin precursors) and the main signal was given based upon uniform asymptotic expansion techniques. Of significant importance, Oughstun [22] proved that the Brillouin precursor can be of significant amplitude when the rise time of the pulse is faster than the relaxation time of the material. This analysis showed that, asymptotically, the Brillouin precursor achieves a peak amplitude at the space-time point $ct/z = n(0)$, where $n(0)$ is the static refractive index of the material, and that the amplitude of this point decays only algebraically as $z^{-1/2}$ with propagation distance z, whereas the amplitudes of the Sommerfeld precursor and the main signal decay exponentially. The relatively slow decay rate of the peak amplitude point of the Brillouin precursor has important practical applications to biomedical imaging as well as to ground- and foliage-penetrating radar systems (see the proceedings series titled *Ultra-Wideband Short-Pulse Electromagnetics* [1, 2, 7, 19, 34, 35]).

The exponential appearing in (1.2) may be written in terms of the complex phase function defined in (1.3) so that, with some algebraic manipulation, the integral representation of the propagated pulse may be expressed as [29]

$$E(z,t) = \frac{1}{2\pi}\Re\left\{ i\int_{ia-\infty}^{ia+\infty} \frac{i}{\omega-\omega_c}\exp\left[\frac{z}{c}\phi(\omega,\theta)\right] d\omega \right\} \tag{1.4}$$

for the input step-function modulated sine wave pulse with fixed carrier frequency $\omega_c > 0$. Because of the exponential appearing in the integrand of (1.4), the Fourier–Laplace representation is ideally suited for analysis by asymptotic expansion techniques that are valid as $z \to \infty$ (i.e., as the propagation distance becomes large), as was originally done by Brillouin. In fact, this problem is much richer in asymptotic theory than the direct application of the method of steepest descent. In order to find a continuous asymptotic approximation to the propagated field $E(z,t)$, three different uniform asymptotic theories are required: a method for two saddle points symmetrically located about the imaginary axis whose real parts are located at plus and minus infinity; a method for two first-order saddle points that coalesce into one second-order saddle point at some fixed space-time point and then separate into first-order saddle points again; and finally, a method for first-order saddle points in the vicinity of a simple pole. These methods have been used extensively by Oughstun and Sherman to study pulse propagation through Lorentz model dielectric materials [21, 25, 26, 27, 28, 29]; their results form the basis of this paper.

The material parameters ($\omega_0 = 4.0\times10^{16}/\text{s}$, $\omega_p^2 = 20.0\times10^{32}/\text{s}^2$, $\delta = 0.28\times10^{16}/\text{s}$) used here are the same as those used by Sommerfeld and Brillouin [6]. The real and imaginary parts of the complex index of refraction $n(\omega)$ for the single-resonance Lorentz model dielectric with these parameters are illustrated in Figure 1.1. This choice of medium parameters corresponds to an extremely absorptive medium. Nev-

a maximum at ω_{SP} and this maximum becomes more pronounced as $z \to \infty$. Hence, the integral appearing in (2.1) may be approximated by the contribution due to a neighborhood of ω_{SP}, the accuracy of this approximation increasing in the sense of Poincaré [31] as $z \to \infty$. This then forms the principle upon which the saddle-point method is based. The saddle-point method may be directly extended to integrals of the type (see Chapter 5 of [29])

$$I(z,\theta) = \int_C f(\omega) \exp\left[z g(\omega,\theta)\right] d\omega, \tag{2.2}$$

in which the position of the saddle point of the exponential function $g(\omega,\theta)$ is a function of the real-valued parameter θ, as is the case in this paper. This is achieved by choosing a path of integration which moves in a continuous manner as θ varies continuously over some specified space-time domain.

3. Behavior of the Complex Phase Function. In order to apply the saddle-point method to the integral appearing in the integral representation (1.4) of the propagated electric field component of a step-function modulated sine wave signal, the behavior of the complex phase function $\phi(\omega,\theta) = i\omega[n(\omega) - \theta]$ must be known in the complex ω-plane [6, 29, 36] as a function of the real parameter θ. For the single-resonance Lorentz model dielectric [18], the complex phase function $\phi(\omega,\theta)$ is analytic in the ω-plane formed by the two branch cuts in the lower half of the ω-plane symmetrically located about the imaginary axis. In the right half plane, the branch cut extends from $\omega_+ \equiv \sqrt{\omega_0^2 - \delta^2} - i\delta$ to $\omega'_+ \equiv \sqrt{\omega_0^2 + \omega_p^2 - \delta^2} - i\delta$.

The saddle points of ϕ are solutions of the equation $\phi_\omega(\omega,\theta) = 0$, which need only be solved for $\theta > 1$ since the field given by (1.4) identically vanishes for all $\theta \le 1$. Brillouin [6] first showed that ϕ possesses two sets of saddle points and provided first-order approximations of the locations of these saddle points; more accurate approximations have since been provided by Oughstun and Sherman [29]. The first set, referred to as the *distant saddle points* and denoted by $\omega_{SP_D^\pm}(\theta)$, consists of two first-order saddle points. As $\theta \to 1^+$,

$$\lim_{\theta \to 1^+} \omega_{SP_D^\pm} \approx \pm\infty - i2\delta, \tag{3.1}$$

while in the opposite limit as $\theta \to \infty$, the distant saddle points approach the outer branch points

$$\lim_{\theta \to \infty} \omega_{SP_D^\pm} \approx \pm\sqrt{\omega_0^2 + \omega_p^2 - \delta^2} - i\delta = \omega'_\pm, \tag{3.2}$$

respectively, so that $|\omega_{SP_D^\pm}(\theta)| \ge \sqrt{\omega_0^2 + \omega_p^2}$ for all $\theta \ge 1$.

The second set of saddle points, referred to as the *near saddle points* and denoted by $\omega_{SP_N^\pm}(\theta)$, consists of two first-order saddle points that lie on the imaginary axis for values of $\theta < \theta_1$, coalesce into a single second-order saddle point when $\theta = \theta_1$, and separate into two first-order saddle points symmetrically located about the imaginary axis for $\theta > \theta_1$, where $\theta_1 \approx \theta_0 + 2\delta^2\omega_p^2/3\theta_0\omega_0^4$, so that $\theta_1 \approx 1.502$ for the material parameters used here. As $\theta \to \infty$, the locations of the near saddle points approach the inner branch points

$$\lim_{\theta \to \infty} \omega_{SP_N^\pm} \approx \pm\sqrt{\omega_0^2 - \delta^2} - i\delta = \omega_\pm, \tag{3.3}$$

respectively. Of particular interest in this evolution is the space-time point $\theta = \theta_0 \equiv n(0)$, where $\theta_0 = 1.5$ for the material parameters considered here, at which the

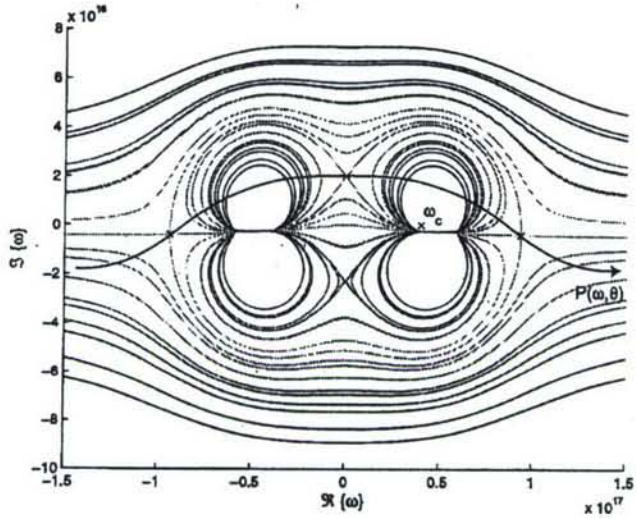

Fig. 3.2 *Contours of $\Re\{\phi(\omega,\theta)\}$ for $\theta = 1.25$ in the complex ω-plane along with an acceptable deformed path of integration $\mathcal{P}(\omega,\theta)$. Notice that the original and deformed contours lie on the same side of the pole.*

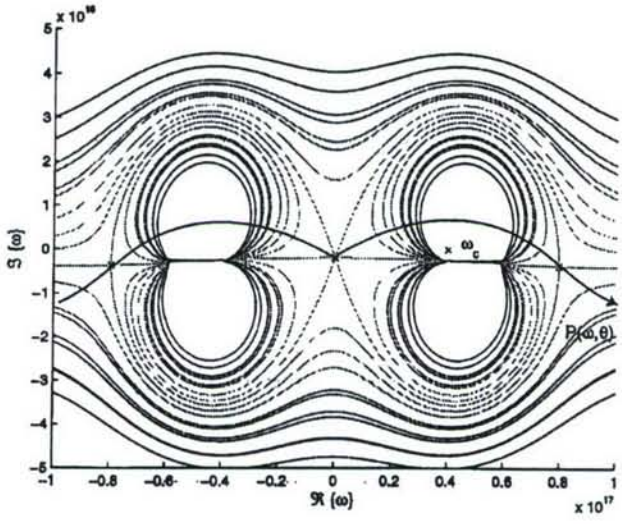

Fig. 3.3 *Contours of $\Re\{\phi(\omega,\theta)\}$ for $\theta = \theta_1$ in the complex ω-plane along with an acceptable deformed path of integration $\mathcal{P}(\omega,\theta)$. Notice that the original and deformed contours lie on the same side of the pole.*

introduced a change of variable such that the saddle points of the transformed phase function retain the limiting values of the original saddle points and then expanded the amplitude function as a finite number of terms plus a remainder term, the remainder term being regular and equal to zero at the saddle points of the transformed phase function. Here, the transformation that retains the essential behavior of the distant saddle points is given by

$$\phi(\omega,\theta) = \alpha_d^2(\theta)s + \beta_d(\theta) + \frac{1}{4s}, \tag{4.1}$$

where $\alpha_d(\theta)$ and $\beta_d(\theta)$ are functions to be determined. The amplitude function is then written as

$$\frac{i}{\omega-\omega_c}\frac{d\omega}{ds} = \gamma_0(\theta) + \gamma_1(\theta)s + \left[\alpha_d^2(\theta) - \frac{1}{4s^2}\right] H_0(s,\theta), \tag{4.2}$$

where $H_0(s,\theta)$ is regular and equal to zero at $s = (\pm 1/\alpha_d)$. Substitution of (4.1) and (4.2) into (1.4) results in the uniform asymptotic description of the Sommerfeld precursor $E_S(z,t)$ for the step-function modulated sine wave [29],

$$\begin{aligned} E_S(z,t) \sim \Re\Big\{ &\exp\left[-i\frac{z}{c}\beta_d(\theta)\right]\left[\gamma_0(\theta)J_0\left(\frac{z}{c}\alpha_d(\theta)\right)\right. \\ &\left.\left. +2\alpha_d(\theta)e^{-i\pi/2}\gamma_1(\theta)J_1\left(\frac{z}{c}\alpha_d(\theta)\right)\right]\right\} + R(z,\theta) \end{aligned} \tag{4.3}$$

as $z \to \infty$ for all $\theta \geq 1$, where $J_n(\xi)$ denotes the Bessel function of the first kind of integer order n. The magnitude of the remainder term is bounded as

$$|R(z,\theta)| \leq K\frac{2c|\alpha_d(\theta)|}{z}\left[\left|J_1\left(\alpha_d(\theta)\frac{z}{c}\right)\right| + \left|J_2\left(\alpha_d(\theta)\frac{z}{c}\right)\right|\right] \tag{4.4}$$

for $z \geq Z > 0$ and $\theta \geq 1$, where $K > 0$ is a constant independent of θ and z. The coefficients appearing in (4.3) are given by

$$\alpha_d(\theta) = \frac{i}{2}\left[\phi(\omega_{SP_D^+},\theta) - \phi(\omega_{SP_D^-},\theta)\right] = -\Im\left\{\phi(\omega_{SP_D^+},\theta)\right\}, \tag{4.5a}$$

$$\beta_d(\theta) = \frac{i}{2}\left[\phi(\omega_{SP_D^+},\theta) + \phi(\omega_{SP_D^-},\theta)\right] = i\Re\left\{\phi(\omega_{SP_D^+},\theta)\right\}, \tag{4.5b}$$

$$\begin{aligned} \gamma_0(\theta) = \frac{1}{2}\Bigg[&\frac{i}{\omega_{SP_D^+}-\omega_c}\left(\frac{1}{2\alpha_d(\theta)}\right)\left(\frac{4\alpha_d^3(\theta)}{i\phi^{(2)}(\omega_{SP_D^+},\theta)}\right)^{1/2} \\ &+\frac{i}{\omega_{SP_D^-}-\omega_c}\left(-\frac{1}{2\alpha_d(\theta)}\right)\left(-\frac{4\alpha_d^3(\theta)}{i\phi^{(2)}(\omega_{SP_D^-},\theta)}\right)^{1/2}\Bigg], \end{aligned} \tag{4.5c}$$

$$\begin{aligned} \gamma_1(\theta) = \frac{1}{4\alpha_d(\theta)}\Bigg[&\frac{i}{\omega_{SP_D^+}-\omega_c}\left(\frac{1}{2\alpha_d(\theta)}\right)\left(\frac{4\alpha_d^3(\theta)}{i\phi^{(2)}(\omega_{SP_D^+},\theta)}\right)^{1/2} \\ &-\frac{i}{\omega_{SP_D^-}-\omega_c}\left(-\frac{1}{2\alpha_d(\theta)}\right)\left(-\frac{4\alpha_d^3(\theta)}{i\phi^{(2)}(\omega_{SP_D^-},\theta)}\right)^{1/2}\Bigg]. \end{aligned} \tag{4.5d}$$

For values of θ bounded away from 1 such that $(z/c)|\alpha_d(\theta)| \gg 1$, the large argument asymptotic expansion of the Bessel function may be substituted into (4.3). This

would be bounded by

$$|R_N| \leq A|z|^{-(2N+\lambda)/2} + B\exp\left[\Re\{z[\phi(\omega_j-,\theta) - g(\omega_i,\theta)]\}\right], \tag{5.1}$$

where A, B are some constants independent of z, and where ω_i is the dominant saddle point while ω_j is the other saddle point, i.e., $\Re\{\omega_i\} < \Re\{\omega_j\}$. Because ω_i is the dominant saddle point, the second term in (5.1) is negligible in comparison to the first, for large enough $|z|$. However, as $\theta \to \theta_1$, $\Re\{\omega_i\} \to \Re\{\omega_j\}$ and $|z|$ must increase without bound in order for the second term in (5.1) to remain negligible compared to the first.

A uniform expansion of the Brillouin precursor, valid for all $\theta > 1$, is obtained through use of the theorem [9, 12, 29] originally due to Chester, Friedman, and Ursell [9]. Here, the transformation that retains the behavior of the saddle points about $\theta = \theta_1$ is given by

$$\frac{1}{3}\nu^3 - \alpha_1(\theta)\nu - \alpha_0(\theta) + \phi(\omega,\theta) = 0, \tag{5.2}$$

where α_0, α_1 are functions to be determined. Note that there are three possible branches of the inverse function. Chester, Friedman, and Ursell [9] proved that only one branch of the transformation defines a conformal mapping of some disc that contains both saddle points. It is this branch which must be used, as shown by Bleistein and Handelsman [4]. As before, the amplitude function is expanded as a finite number of terms plus a remainder that is regular and equal to zero at the transformed saddle points. This is obtained using the expansion

$$\frac{i}{\omega-\omega_c}\frac{d\omega}{d\nu} \equiv G_0(\nu,\theta) = h_1(\theta) + h_2(\theta)\nu + (\nu^2 - \alpha_1(\theta))H_0(\nu,\theta), \tag{5.3}$$

where h_1, h_2, and H_0 are to be determined. Substitution of (5.2) and (5.3) into (1.4) results in the uniform asymptotic expansion of the Brillouin precursor $E_B(z,t)$ for the step-function modulated sine wave [29]

$$\begin{aligned} E_B(z,t) = -\Re\Bigg\{ &\exp\left[\frac{z}{c}\alpha_0(\theta)\right]\Bigg\{\left(\frac{c}{z}\right)^{1/3} e^{-i2\pi/3}\cdot Ai\left(\alpha_1(\theta)\, e^{-i2\pi/3}\left(\frac{c}{z}\right)^{2/3}\right) \\ &\cdot\left\{\frac{1}{2}\left[\frac{i}{\omega_{SP_N^+}-\omega_c}h_+(\theta) + \frac{i}{\omega_{SP_N^-}-\omega_c}h_-(\theta)\right] + \mathcal{O}\left(\frac{1}{z}\right)\right\} \\ &+\left(\frac{c}{z}\right)^{2/3} e^{-i2\pi/3}Ai^{(1)}\left(\alpha_1(\theta)\, e^{-i2\pi/3}\left(\frac{c}{z}\right)^{2/3}\right) \\ &\cdot\left\{\frac{1}{2\alpha_1^{1/2}(\theta)}\left[\frac{i}{\omega_{SP_N^+}-\omega_c}h_+(\theta) - \frac{i}{\omega_{SP_N^-}-\omega_c}h_-(\theta)\right] + \mathcal{O}\left(\frac{1}{z}\right)\right\}\Bigg\}\Bigg\}, \end{aligned} \tag{5.4}$$

where $Ai(\xi)$ denotes the Airy function and the coefficients appearing in (5.4) are given by

$$\alpha_0(\theta) = \frac{1}{2}\left[\phi(\omega_{SP_N^+},\theta) + \phi(\omega_{SP_N^-},\theta)\right], \tag{5.5a}$$

$$\alpha_1^{1/2}(\theta) = \left\{\frac{3}{4}\left[\phi(\omega_{SP_N^+},\theta) - \phi(\omega_{SP_N^-},\theta)\right]\right\}^{1/3}, \tag{5.5b}$$

$$h_\pm(\theta) = \left(\mp\frac{2\alpha_1^{1/2}(\theta)}{\phi^{(2)}(\omega_{SP_N^+},\theta)}\right)^{1/2} \tag{5.5c}$$

total field evolution as $z \to \infty$. The instantaneous angular frequency of oscillation of the Brillouin precursor starts at zero when $\theta = \theta_1$ and monotonically increases to approach the value $\sqrt{\omega_0^2 - \delta^2}$ with increasing θ.

Previous work [29, 36] exhibited a discontinuity in the uniform asymptotic approximation of the Brillouin precursor about the space-time point $\theta = \theta_1$, which the authors attributed to numerical instabilities. These numerical instabilities are now known to be caused by the use of an unnecessary approximation of the lower near saddle-point location $\omega_{SP_N^-}(\theta)$ and incorrect phase values for the coefficients $h_\pm(\theta)$ for all $\theta > \theta_1$. Here, all saddle-point locations and coefficients are numerically determined so that this approximation error is avoided, resulting in a continuous evolution of the Brillouin precursor for all $\theta > 1$.

6. The Signal Contribution. The signal contribution to the propagated field of the step-function modulated sine wave is due to the simple pole singularity at $\omega = \omega_c$ appearing in the integrand of (1.4). It is assumed here that ω_c is real, positive, and finite (as all physical frequencies must be). The simple pole located at ω_c may influence the value of $E(z,t)$ if the path $\mathcal{P}(\omega,\theta)$ crosses the pole singularity, or if either of the saddle points $\omega_{SP_{D,N}^+}(\theta)$ comes within close proximity of the pole, or both.

Let the path $\mathcal{P}(\omega,\theta)$ comprise the portions of the steepest descent paths emanating from $\omega_{SP_N^+}(\theta)$ and $\omega_{SP_D^+}(\theta)$ and continuing into the upper half plane. In the deformation of the original path of integration appearing in (1.4) into the path $\mathcal{P}(\omega,\theta)$, the simple pole located at ω_c is crossed at some space-time point $\theta = \theta_s \geq 1$. Hence, the original integral and the integral

$$E_{SDP}(z,t) = \frac{1}{2\pi}\Re\left\{ i \int_{\mathcal{P}(\omega,\theta)} \frac{i}{\omega - \omega_c} \exp\left[\frac{z}{c}\phi(\omega,\theta)\right] d\omega \right\} \tag{6.1}$$

along the deformed contour are related by

$$E(z,t) = E_{SDP}(z,t) \qquad \text{for } \theta < \theta_s, \tag{6.2a}$$

$$E(z,t) = E_{SDP}(z,t) - \pi i \gamma e^{(z/c)\phi(\omega_c,\theta_s)} \qquad \text{for } \theta = \theta_s, \tag{6.2b}$$

$$E(z,t) = E_{SDP}(z,t) - 2\pi i \gamma e^{(z/c)\phi(\omega_c,\theta)} \qquad \text{for } \theta > \theta_s, \tag{6.2c}$$

where

$$\gamma = \lim_{\omega \to \omega_c} (\omega - \omega_c) \frac{i}{\omega - \omega_c} = i \tag{6.3}$$

is the residue of the amplitude function at the simple pole ω_c. Direct application of the saddle-point method to $E_{SP}(z,t)$ yields a uniform expansion. However, it does not provide a uniform expansion for $E(z,t)$. In order to see this, let θ_c denote the space-time point at which the pole becomes dominant over the saddle point ω_{SP} in the sense that $\Re\{\phi(\omega_c,\theta)\} > \Re\{\phi(\omega_{SP},\theta)\}$. Because the path $\mathcal{P}(\omega,\theta)$ lies in the valleys of ω_{SP}, it necessarily follows that $\theta_s < \theta_c$. From (6.2), it is obvious that $E(z,t)$ changes discontinuously about $\theta = \theta_s$ when the saddle-point method is applied to $E_{SDP}(z,t)$. However, because the simple pole lies in the valley of the saddle point, the residue contributions appearing in (6.2) are exponentially smaller than $E_{SDP}(z,t)$ and pose no problem in obtaining a uniform approximation to $E(z,t)$. This is not the case at $\theta = \theta_c$ when the simple pole ω_c becomes dominant over the saddle point ω_{SP}. Here, $\Re\{\phi(\omega_{SP},\theta)\} < \Re\{\phi(\omega_c,\theta)\}$ for $\theta_s < \theta < \theta_c$ and the

while θ_s and the appropriate residue contribution are determined by the saddle point whose path of steepest descent crosses the simple pole located at ω_c. The space-time point θ_s at which the path $\mathcal{P}(\omega,\theta)$ crosses the simple pole located at ω_c is determined by the equation

$$Y(\omega_c,\theta_s) = Y(\omega_{SP},\theta_s), \tag{6.7}$$

where $Y \equiv \Im\{\phi\}$ and ω_{SP} denotes either $\omega_{SP_N^+}(\theta)$ or $\omega_{SP_D^+}(\theta)$. We have found (by inspection) that the deciding factor as to which saddle point determines the value of θ_s is the value of $Y(\omega_c,\theta)$ at $\theta = 1$. If $Y(\omega_c,1) > 0$, the steepest descent path emanating from the near saddle point $\omega_{SP_N^+}(\theta)$ is used to determine the value θ_s. If $Y(\omega_c,1) < 0$, the steepest descent path emanating from the distant saddle point $\omega_{SP_D^+}(\theta)$ is used to determine the value θ_s. If $Y(\omega_c,1) = 0$, then $\theta_s = 1$. The value of $\omega_c = \omega_Y$ which separates the two cases is given approximately by $\omega_Y \approx 4.2925 \times 10^{16}$ rad/s for the material parameters considered here. As a consequence, we have applied the uniform theory to account for two first-order saddle points with a nearby simple pole singularity. As an example, for angular frequencies ω_c satisfying $Y(\omega_c,1) > 0$, the uniform signal contribution is given by

$$\begin{aligned} E_c(z,t) = \frac{1}{2\pi}\Re\Bigg\{ & i\gamma_u\left[-i\pi \operatorname{erfc}\left(i\Delta_D(\theta)\sqrt{\frac{z}{c}}\right)\exp\left[\frac{z}{c}\phi(\omega_c,\theta)\right]\right. \\ & \left. + \frac{1}{\Delta_D(\theta)}\sqrt{\frac{\pi c}{z}}\exp\left[\frac{z}{c}\phi(\omega_{SP_D^+},\theta)\right]\right] \\ & + i\gamma_u\left[-i\pi \operatorname{erfc}\left(i\Delta_N(\theta)\sqrt{\frac{z}{c}}\right)\exp\left[\frac{z}{c}\phi(\omega_c,\theta)\right]\right. \\ & \left.\left. + \frac{1}{\Delta_N(\theta)}\sqrt{\frac{\pi c}{z}}\exp\left[\frac{z}{c}\phi(\omega_{SP_N^+},\theta)\right]\right]\right\}, \qquad \theta < \theta_s, \end{aligned} \tag{6.8a}$$

$$\begin{aligned} E_c(z,t) = \frac{1}{2\pi}\Re\Bigg\{ & i\gamma_u\left[-i\pi \operatorname{erfc}\left(i\Delta_D(\theta)\sqrt{\frac{z}{c}}\right)\exp\left[\frac{z}{c}\phi(\omega_c,\theta)\right]\right. \\ & \left. + \frac{1}{\Delta_D(\theta)}\sqrt{\frac{\pi c}{z}}\exp\left[\frac{z}{c}\phi(\omega_{SP_D^+},\theta)\right]\right] \\ & + i\gamma_u\left[i\pi \operatorname{erfc}\left(-i\Delta_N(\theta)\sqrt{\frac{z}{c}}\right)\exp\left[\frac{z}{c}\phi(\omega_c,\theta)\right]\right. \\ & \left.\left. + \frac{1}{\Delta_N(\theta)}\sqrt{\frac{\pi c}{z}}\exp\left[\frac{z}{c}\phi(\omega_{SP_N^+},\theta)\right]\right]\right\} + \Re\left\{i\exp\left[\frac{z}{c}\phi(\omega_c,\theta)\right]\right\}, \qquad \theta \geq \theta_s, \end{aligned} \tag{6.8b}$$

as $z \to \infty$. Here, $\gamma_u = i$ is the residue of the amplitude function $i(\omega - \omega_c)$ at ω_c, $\operatorname{erfc}(\xi)$ is the complementary error function, and

$$\Delta_{D,N}(\theta) \equiv \left[\phi(\omega_{SP_{D,N}^+},\theta) - \phi(\omega_c,\theta)\right]^{1/2}. \tag{6.9}$$

A similar expression may be given for the uniform signal contribution for carrier frequencies ω_c satisfying $Y(\omega_c,1) > 0$ [8].

Questions about the accuracy of this uniform expansion as it applies to the classical problem of a step-function modulated sine wave signal have persisted because, until now, it has been difficult to isolate the leading edge of the pole contribution from the remainder of the field. For all values of ω_c, either the Sommerfeld or the

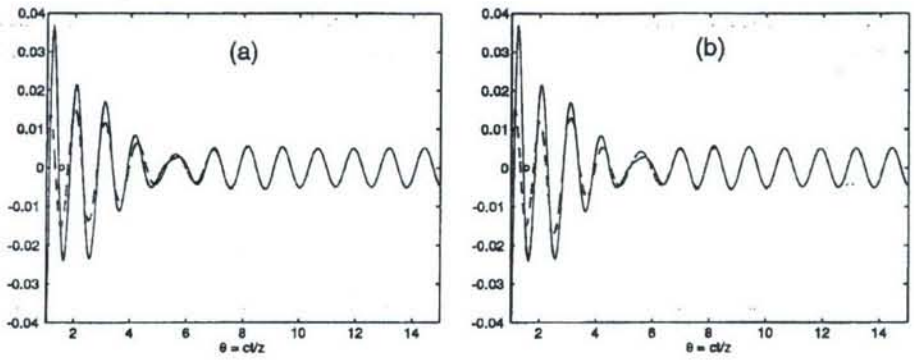

Fig. 6.2 *Comparison of asymptotic (dashed curve) and numerical (solid curve) pole contributions for a step-function modulated sine wave with intra-absorption band frequency* $\omega_c = 1.25\omega_0$ *at an observation distance of* $z \approx 5.3z_d$. *The asymptotic approximation is made* (a) *utilizing only the distant saddle point* $\omega_{SP_D^+}(\theta)$, *and* (b) *utilizing both saddle points* $\omega_{SP_D^+}(\theta)$ *and* $\omega_{SP_N^+}(\theta)$.

at a propagation distance of $z \approx 5.3z_d$. In Figure 6.2 (b), the asymptotic approximation of the pole contribution (dashed curve) is calculated using both $\omega_{SP_N^+}(\theta)$ and $\omega_{SP_D^+}(\theta)$. The open circle denotes the space-time value θ_s when the path $\mathcal{P}(\omega, \theta)$ crosses ω_c. A comparison of the two figures shows that the contribution from the near saddle point $\omega_{SP_N^+}(\theta)$ is minimal. However, these figures again confirm that the uniform asymptotic theory provides the correct approximation to the pole contribution. This is in contrast to the previous hypothesis [29] that both saddle points $\omega_{SP_D^+}(\theta)$ and $\omega_{SP_N^+}(\theta)$ are sufficiently removed from ω_c when ω_c is within the absorption band of the material so that $E_c(z,t)$ is composed solely of the residue term which abruptly begins at $\theta = \theta_s$.

7. Conclusions. The propagated electric field component of a linearly polarized, plane-wave, step-function modulated sine wave signal of applied carrier frequency ω_c traveling through a single-resonance Lorentz dielectric has been studied in this paper. An analytic, asymptotic approximation of the propagated wave field requires the application of three uniform theories in the subject of asymptotic expansions of integrals. The results presented here provide the first correct description of the pole contribution of the field (1.4) for applied carrier frequencies that lie within and above the absorption band of the material. Previous attempts to isolate the pole contribution from the rest of the field were unsuccessful due to inaccurate asymptotic results for the Brillouin precursor about the space-time point $\theta = \theta_1$ and an incorrect asymptotic representation of the pole contribution for applied carrier frequencies in the range $\omega_c > \sqrt{\omega_0^2 + \omega_p^2 - \delta^2}$.

Four different carrier frequencies of the step-function modulated sine wave signal were considered in this paper: the below-resonance carrier frequency $\omega_c = 0.5\omega_0$, the intra-absorption band carrier frequencies $\omega_c = \omega_0$ and $\omega_c = 1.25\omega_0$, and the above-resonance carrier frequency $\omega_c = 2.5\omega_0$. The total asymptotic field, which is the sum of the three asymptotic components, $E(z,t) = E_S(z,t) + E_B(z,t) + E_c(z,t)$, is presented for each applied carrier frequency as the dashed curves in the upper plots of Figures 7.1–7.4. The solid curves appearing in these figures represent the

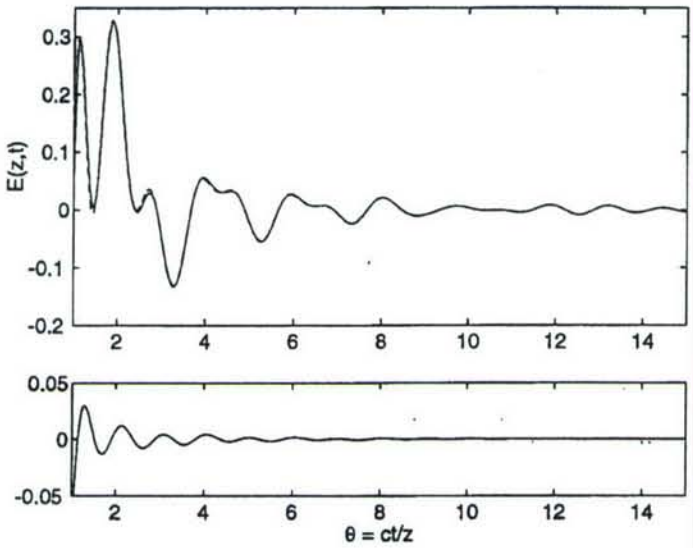

Fig. 7.3 *The total asymptotic (dashed curve) and numerical (solid curve) fields of the step-function modulated sine wave signal with intra-absorption band applied carrier frequency* $\omega_c = 1.25\omega_0$ *rad/s at a distance of* $z = 3 \times 10^{-8}$ $m \approx 5.3z_d$ *into the single-resonance Lorentz dielectric. The lower figure shows the difference between the two results.*

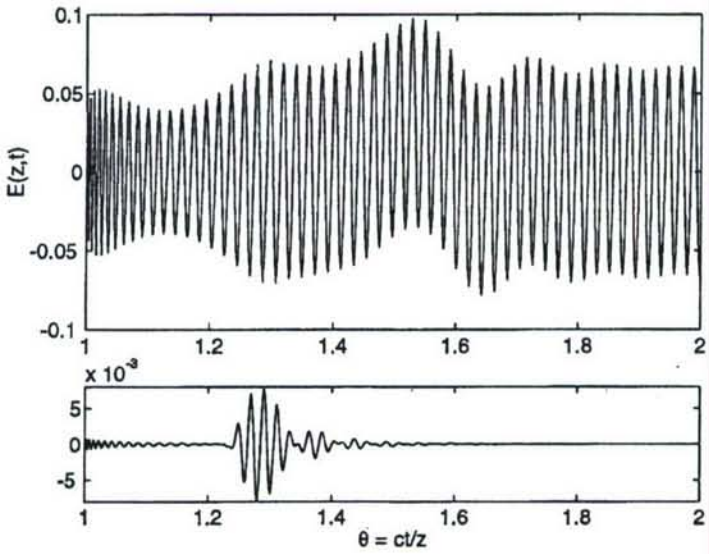

Fig. 7.4 *The total asymptotic (dashed curve) and numerical (solid curve) fields of the step-function modulated sine wave signal with above-absorption band applied carrier frequency* $\omega_c = 2.5\omega_0$ *at a distance of* $z = 9 \times 10^{-7}$ $m \approx 2.7z_d$ *into the single-resonance Lorentz dielectric. The lower figure shows the difference between the two results.*

[18] H. A. LORENTZ, *The Theory of Electrons*, Teubner, Leipzig, 1906.
[19] E. MOKOLE, M. KRAGALOTT, AND K. GERLACH, EDS., *Ultra-Wideband, Short-Pulse Electromagnetics* 6, Springer, New York, 2003.
[20] H. M. NUSSENZVEIG, *Causality and Dispersion Relations*, Academic Press, New York, 1972.
[21] K. E. OUGHSTUN, *Pulse propagation in a linear, causally dispersive medium*, IEEE Proc., 79 (1991), pp. 1394–1420.
[22] K. E. OUGHSTUN, *Noninstantaneous, finite, rise-time effects on the precursor field formation in linear dispersive pulse propagation*, J. Opt. Soc. Amer. A, 12 (1995), pp. 1715–1729.
[23] K. E. OUGHSTUN AND N. A. CARTWRIGHT, *On the Lorentz-Lorenz formula and the Lorentz model of dielectric dispersion*, Opt. Exp., 11 (2003), pp. 1541–1546.
[24] K. E. OUGHSTUN AND N. A. CARTWRIGHT, *On the Lorentz-Lorenz formula and the Lorentz model of dielectric dispersion: Addendum*, Opt. Exp., 11 (2003), pp. 2791–2792.
[25] K. E. OUGHSTUN AND G. C. SHERMAN, *Optical pulse propagation in temporally dispersive Lorentz media*, J. Opt. Soc. Amer., 65 (1975), p. 1224A.
[26] K. E. OUGHSTUN AND G. C. SHERMAN, *Uniform asymptotic description of dispersive pulse propagation*, J. Opt. Soc. Amer. A, 69 (1979), p. 1448A.
[27] K. E. OUGHSTUN AND G. C. SHERMAN, *Uniform asymptotic description of electromagnetic pulse propagation in a linear dispersive medium with absorption (the Lorentz medium)*, J. Opt. Soc. Amer. A, 6 (1989), pp. 1394–1420.
[28] K. E. OUGHSTUN AND G. C. SHERMAN, *Uniform asymptotic description of ultrashort rectangular optical pulse propagation in a linear, causally dispersive medium*, Phys. Rev. A, 41 (1990), pp. 6090–6113.
[29] K. E. OUGHSTUN AND G. C. SHERMAN, *Pulse Propagation in Causal Dielectrics*, Springer, Berlin, 1994.
[30] O. PERRON, *Über die näherungsweise Berechnung von Funktionen großber Zahlen*, Sitzungsber. Bayr. Akad. Wissensch., (1917), pp. 191–219.
[31] H. POINCARÉ, *Sur les integrals irregulieres des equations lineaires*, Acta Math., 8 (1886), pp. 295–344.
[32] L. RAYLEIGH, *On progressive waves*, Proc. London Math. Soc., 9 (1877), pp. 21–26.
[33] B. RIEMANN, *Riemann's "gesammelte mathematische werke,"* 2nd ed., Zweite Auflage, 1892, pp. 424–430. (This paper, dated October 1863, was reconstructed from notes by H. A. Schwarz.)
[34] J. SHILOH, B. MANDELBAUM, AND E. HEYMAN, EDS., *Ultra-Wideband, Short-Pulse Electromagnetics* 4, Springer, New York, 1999.
[35] P. SMITH AND S. CLOUDE, EDS., *Ultra-Wideband, Short-Pulse Electromagnetics* 5, Springer, New York, 2002.
[36] J. A. SOLHAUG, K. E. OUGHSTUN, J. J. STAMNES, AND P. D. SMITH, *Uniform asymptotic description of the Brillouin precursor in a single-resonance Lorentz model dielectric*, Pure Appl. Opt., 7 (1998), pp. 575–602.
[37] A. SOMMERFELD, *Über die fortpflanzung des lichtes in disperdierenden medien*, Ann. Phys., 44 (1914), pp. 177–202.
[38] J. A. STRATTON, *Electromagnetic Theory*, McGraw-Hill, New York, 1941.
[39] E. T. WHITTAKER AND G. N. WATSON, *A Course of Modern Analysis*, Macmillan, New York, 1943, section 5.2.
[40] P. WYNS, D. P. FOTY, AND K. E. OUGHSTUN, *Numerical analysis of the precursor fields in linear dispersive pulse propagation*, J. Opt. Soc. Amer. A, 6 (1988), pp. 1421–1429.
[41] H. XIAO AND K. E. OUGHSTUN, *Failure of the group-velocity description for ultrawideband pulse propagation in a causally dispersive, absorptive dielectric*, J. Opt. Soc. Amer. B, 16 (1999), pp. 1773–1785.

AU: See query